2024

COMPUTATIONAL EVALUATION OF SOME BASIC MATERIAL PARAMETERS IN COBALT-ALUMINUM ALLOYS

Hemanth Kumar Reddy Basireddy
Michigan Technological University, hbasired@mtu.edu

COMPUTATIONAL EVALUATION OF SOME BASIC MATERIAL PARAMETERS IN COBALT-ALUMINUM ALLOYS

By

Hemanth Kumar Reddy Basireddy

A THESIS

Submitted in partial fulfillment of the requirements for the degree of

MASTER OF SCIENCE

In Materials Science and Engineering

MICHIGAN TECHNOLOGICAL UNIVERSITY

2024

This thesis has been approved in partial fulfillment of the requirements for the Degree of MASTER OF SCIENCE in Materials Science and Engineering.

Department of Materials Science and Engineering

Thesis Advisor:	*Yu Wang*
Committee Member:	*Stephen Kampe*
Committee Member:	*Walter W. Milligan*
Department Chair:	*Walter W. Milligan*

Table of Contents

Author Contribution Statement

The research idea was proposed by my advisor, Dr. Yu Wang. Dr. Yu Wang developed the theoretical formalism and the candidate performed numerical simulations and analytic calculations. All authors discussed the results and contributed to the final manuscript.

Acknowledgements

I express my deepest and sincere gratitude to my advisor Dr. Yu Wang for his constant support, friendly guidance, and patience. His advice and encouragement helped me keep going throughout this investigation. I would like to thank Dr. Yongmei Jin for her help and support whenever there is a problem in the process of conducting my research. I also thank Dr. Liwei Geng for his support in conducting VASP simulations. I appreciate and thank my parents for their emotional support and encouragement in completing the thesis.

The High-Performance Computing Shared Facility (Superior) at Michigan Technological University was used in obtaining results presented in this Thesis.

Abstract

The First Principles Density Functional Theory study is conducted on BCC Co-Al based solid solution which obeys Vegard's law. Chemical bond energies are calculated beyond 1NN interactions as second-nearest-neighbor and third-nearest-neighbor chemical bond energy values are significant and contribute to the total energy of the alloy. Elastic energy developed in the alloys due to the atomic radius misfit between solute and solvent atoms is also considered. Effects of atomic ordering on 1NN, 2NN, and 3NN chemical ordering energies and lattice parameters are investigated.

1 Introduction

In Japan, in the early ‘60s attempt to discover new permanent magnets led to the discovery of magnetic alloys with high coercivity based on β-phase CoAl intermetallic compounds and it was found that magnetic Al-Co alloys containing more than 10% aluminum show high coercive forces and thus the investigators named these alloys “Malcolloy” [1].

Frenkel and Dorfman [2] recognized that energetically it is unfavorable for domain wall formation when ferromagnetic particle size is below a critical size. Magnetic properties of fine-particle Permanent magnets are attained through a microstructure that consists of small, single-domain ferromagnetic particle assemblies that are dispersed in a weak ferromagnetic or non-magnetic matrix. Livingston [3] concluded that high coercivity of hard magnetic materials could be achieved only by changing intrinsic properties such as crystal anisotropy. Further development confirmed that coercivity is controlled by domain processes in high crystal anisotropy-based permanent magnets [4]. Hence relationship between microstructure and coercivity of fine particle permanent particles is established. In the early 1970s research on Co-Al-based magnetic alloys peaked, examining various aspects of magnetic properties and phase transformation mechanisms in these alloys [5]. Investigators involved in the study proposed different phase transformation mechanisms but all of them concluded that magnetic hardening of Co-Al-based alloys results from aged microstructure which consists of elongated single-domain ferromagnetic particle assembly dispersed in a weak ferromagnetic or paramagnetic matrix. A.M. Zeltser et al [6] study on Co-Al alloys indicates that during aging Co-rich β-

CoAl matrix precipitates elongated single-domain fine-particles which produce different microstructure entirely with corresponding magnetic behavior. As these studies indicate the potential of Co-Al-based permanent magnets, Malcolloy's high coercivity is believed to be dependent on magneto crystalline anisotropy at room temperature [7] whereas other alloys namely Chromindur, Cunife, Cunico, and Alnico obtain high coercivity as a result of high resistance to magnetization reversal. Schwartz [5] investigated Co-24.8 wt.% Al β-phase alloys in an attempt to correlate specific magnetic properties development with the evolution of microstructure using conventional and high-resolution transmission electron microscopy, magnetic measurements, and electron diffraction. The investigation shows that coercivity development follows microstructure evolution.

This thesis focuses on Co-rich off-stoichiometric β-CoAl alloys. Figure 1.1 shows the Co-rich portion of the Co-Al equilibrium phase diagram with superimposed Curie temperatures for the ferromagnetic transition of β-CoAl and α-Co phases [8]. Upon quenching the solution from treatment temperature, B2 ordering of various degrees is achieved in the supersaturated β-CoAl substitutional solid solution. The magnetic properties of the partially ordered off-stoichiometric β-CoAl alloys can be studied computationally by employing an atomistic spin model [9]. In such a model, the spin dynamics of atomic moments at a system of atomic sites are simulated by solving the atomistic Landau-Lifshitz-Gilbert equation [10]. The atomic sites are inputs from an atomic configuration that is predetermined. To determine the atomic configuration of the interested system, the atomistic Monte Carlo method has been developed in our group

[11], which takes the chemical interactions of neighboring atoms and elastic interactions arising from atomic radius misfit between solute and solvent atoms into account. This method was employed to study substitutional Fe-Ga alloys, where relevant material input parameters are determined from First-Principles Density Functional Theory calculations [11]. To determine atomic configurations of interest in the partially ordered off-stoichiometric β-CoAl alloys, the same atomistic Monte Carlo method will be employed. However, to do so, the relevant material input parameters of β-CoAl alloys need to be determined first. The purpose of this research is to determine some basic material parameters for the Co-rich Co-Al substitutional solid solutions by First-Principles within the framework of Density Functional Theory implemented in the Vienna Ab initio Simulation Package. The simulations are run on Michigan Technological University's Superior supercomputer.

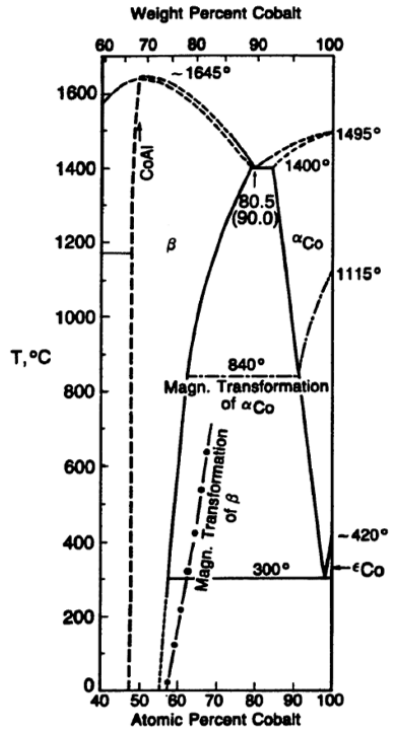

Figure 1.1. The Co-Al equilibrium phase diagram of Co rich portion [12] that is superimposed with Curie temperatures of the β-CoAl [13] and α-Co phases for a ferromagnetic transition

2 Hypotheses and Tests

A proposition is made to determine basic material parameters in the Co-rich Co-Al substitutional solid solutions which are chemical bond energies up to the third nearest neighbors and elastic energy due to atomic radius misfit between solvent Co and solute Al atoms.

2.1 Chemical Energy: First, Second, and Third Nearest Neighbor Bonds

The conventional regular solid solution model considers only first nearest neighbor (1NN) bonds, which are assumed to dominate over other bonds of longer distances. In this study bonds up to the third nearest neighbors are considered and bond energies at different compositions(x) of the alloy $Co_{1-x}Al_x$ are calculated.

2.1.1 Significance of Second and Third Nearest Neighbor Bonds

To describe the properties of a wide range of alloys, the first nearest neighbor(1NN) atomic interactions are considered. However, due to shortcomings in predicting the energy of the lattice, properties, and stability for some BCC structure alloys, Lee et al. [14] considered second-nearest neighbor (2NN) interactions for BCC Fe metal. Calculated properties considering 2NN interactions are compared with experimental data and results are found to be satisfactory. Lee et al. [15] further extended the study to find the properties of BCC transition metals. Following [15], Zhiwei et al. [16] demonstrated

that the potential developed for lithium-silicon (Li-Si) alloys considering 2NN interactions is capable of predicting material properties. Jeong et al. [17] investigated binary systems considering 2NN interactions, the interatomic potential was found to reproduce various fundamental properties that are in good agreement with the experimental values.

Soren et al. [18] investigation shows that considering only 1NN interactions fails to predict key magnetic and electronic properties, and including a third nearest neighbor (3NN) interactions gives accurate results. For the β-CoAl solid solution which is considered for this study chemical energies up to the third nearest neighbor are considered. The role of 1NN and 2NN interactions in understanding the decomposition paths and microstructure evolution is analyzed by Soffa et al. [19]. Thermodynamic stability and energetics of binary alloys are discussed in terms of 1NN pairwise interaction energies and the sign of chemical ordering energy (**Ω**) which is given by the below equation.

Eq. 2.1 $$\Omega = E_{Co-Al} - \left(E_{Co-Co} + E_{Al-Al}\right)/2$$

Ω is 1NN chemical ordering energy, $E_{Co\text{-}Co,}$ $E_{Al\text{-}Al,}$ and $E_{Co\text{-}Al}$ are the bond energies of Co-Co, Al-Al, and Co-Al. According to the investigation [19] for **Ω** < 0, $E_{Co\text{-}Al} < (E_{Co\text{-}Co} + E_{Al\text{-}Al})/2$, favoring of unlike pairs occurred, and the system was classified as ordering. And for **Ω**>0, $E_{Co\text{-}Al} > (E_{Co\text{-}Co} + E_{Al\text{-}Al})/2$, Co-Co and Al-Al bonds are preferred within the solid solution. The pairwise interaction is extended to 2NN interactions and the 2NN chemical ordering energy (**Ω**') is given by the equation

Eq. 2.2 $$\Omega' = E'_{Co-Al} - \left(E'_{Co-Co} + E'_{Al-Al}\right)/2$$

$E'_{Co\text{-}Al}$, $E'_{Co\text{-}Co,}$ and $E'_{Al\text{-}Al}$ are bond energies associated with 2NN interaction energies.

Similarly, 3NN interchange energy (Ω'') is given by the equation

Eq. 2.3 $$\Omega'' = E''_{Co-Al} - \left(E''_{Co-Co} + E''_{Al-Al}\right)/2$$

$E''_{Co-Al}, E''_{Co-Co} and\ E''_{Al-Al}$ are the energy values corresponding to 3NN bonds.

Chemical bond energy calculations of β-CoAl are done using VASP. 3*3*3 BCC supercell is used for the simulations. Unit cell lattice parameter extrapolated from Vegard's plot of β-CoAl shown in chapter 4.3.3 is used as the unit cell lattice parameter for 3*3*3 supercell and the Co and Al atoms in the supercell are considered to be in the fixed state for the simulation. The chemical ordering energies calculated are compared with each other to interpret the significance of 2NN and 3NN compared to 1NN energy. The aluminum composition x=2/54 for the alloy $Co_{1-x}Al_x$ is considered for calculating 1NN, 2NN, and 3NN bond energies. For $Co_{52}Al_2$ alloy changing one of the Al atomic positions in the supercell by keeping another in a fixed position, the respective chemical bond energies are calculated.

2.1.2 Dependence of Bond Energy on Alloy Composition

Chemical bond energies considering 1NN, 2NN, and 3NN interactions of $Co_{1-x}Al_x$ are calculated for x=4/54=0.07407 ($Co_{50}Al_4$) similar to the $Co_{52}Al_2$ alloy using 3*3*3

supercell VASP simulations with the same input parameters and extrapolated unit cell lattice parameter value. For x=4/16=0.25 ($Co_{12}Al_4$) 1NN, 2NN, and 3NN chemical bond energies are calculated by exchanging the Al atomic positions with Co atoms in DO_3 ordered structure. The simulations for $Co_{12}Al_4$ are performed using VASP and 2*2*2 supercell is used for this case of bond energy calculations and the lattice parameter used for this case is the same unit cell extrapolated lattice parameter from Vegard's linear plot.

Using 2*2*2 supercell 1NN, 2NN, and 3NN chemical bond energies for x=2/16=0.125 ($Co_{14}Al_2$) are calculated by changing the atomic positions of aluminum atoms. Bond energies for x=0.5 are also calculated by exchanging the aluminum atomic positions with Co atoms in the B2 and B32 ordered phases. The 1NN, 2NN, and 3NN energy calculations of $Co_{52}Al_2$, $Co_{50}Al_4$, $Co_{12}Al_4$, $Co_{14}Al_2$, and Co_8Al_8 i.e., for x = 0.037, 0.07407, 0.125, 0.25, and 0.5 respectively are compared to show the values are not constant and are composition dependent.

2.2 Elastic Energy: Vegard's Law and Atomic Radius Misfit

The conventional regular solid solution model considers chemical energy and entropy but does not include elastic energy associated with the crystal lattice distortion caused by the different atomic radii of solute and solvent atoms. This study includes elastic energy which is calculated from Vegard's plot of β-CoAl.

2.2.1 Validation of Vegard's Law in Co-Al BCC-based Solid Solution

Crystal structure analysis by applying X-ray diffraction on several ionic salt alloys showed an observation that at constant temperature, there exists a linear relationship between crystal lattice parameter and concentration of alloy constituents. This empirical rule is named as Vegard's law [20]. However, when extended to metallic alloys, studies showed that a majority of them do not obey the rule [21]. Further studies investigated the relationship between the crystal lattice constant of alloys and the concentration of the binary components. Among those, First Principles Density Functional Theory has also been used to find out if any such relationship exists and if it exists what are the factors that affect the relationship. A brief discussion on the First Principles Density Functional Theory of classical non-uniform fluid mixtures and its relationship with Vegard's law has been reported [22]. According to [23], identifying physical factors that affect the crystal structure of alloys can be done readily, which include: firstly, geometric differences in alloy constituent element's atomic sizes, Secondly, in pure element crystals, the relative volume per valence electrons, third, the Brillouin-zone effects, and lastly, Electro-chemical differences between the alloy constituent's elements. The significance of atomic size difference in determining crystal structure and lattice constant of a simple binary alloy is established by applying the Density Functional Theory of non-uniform fluid mixtures of hard spheres [24]. It is also proposed that DFT applied to fluid–solid transition of non-uniform fluid mixtures that are simple binary mixtures of hard spheres demonstrates the importance of relative atomic sizes in determining crystal structure, the

lattice parameters of alloys, and also the lattice constant and concentration relationship dependence on relative atomic sizes. It is also suggested that Vegard's law may hold along the fluid-solid coexistence curve for small atomic size disparities between the two elements which are the constituents of the alloy.

In this study, atomistic modeling of super saturated CoAl BCC-based solid solution is investigated using VASP (Vienna Ab-initio Simulation Package) which performs a quantum mechanical calculation based on First Principles Density Functional Theory. For the 2*2*2 supercell which consists of 8-unit cells of BCC structure with Co and Al occupying the atomic positions. VASP simulation is used to determine lattice parameters for different compositions of Aluminum i.e., the composition of Al in CoAl BCC-based structure varying from 0 At. % to 50 At.%. After lattice parameters of BCC-based Co-Al for different Al compositions (x) in $Co_{1-x}Al_x$ are calculated, data is fitted to Vegard's law, which manifests the elasticity effect and can be used to determine the atomic radius misfit between Co and Al atoms. Thus, DFT calculation results establish, a relationship between the lattice constant of alloy and the composition of Al.

2.2.2 Elastic Energy of Co-Al BCC-Based Solid Solution

Lattice distortions induced in a substitutional solid solution due to atomic radius misfit between solute and solvent were studied based on First Principles [25]. The misfit strain and misfit parameter introduced in the lattice due to atomic radius misfit in various solid solutions have also been studied using the first principles [26]. The strength of alloys

affected by atomic radius misfit is presented in [27]. The above studies show the significance of elastic energy in the solid solution induced due to atomic radius misfit. Microelasticity Theory [28] is used for calculating the elastic energy of a solid solution. Microelasticity theory is widely used in material science for developing computational models to determine and study microstructure evolution and strengthening mechanisms of different alloys under different conditions [29]. Elastic energy and magnetostatic energy effects on magnetic domains are studied by proposing a computational model for magnetostrictive materials by combining a micromagnetic model with the phase field microelasticity theory [30]. The computational model also predicts an increase in magnetostrictive effect under compressive pre-stress. As elastic energy affects magnetic properties, for β-CoAl solid solution elastic energy is also considered along with chemical energy [11]. For calculating the elastic energy linear equation of Vegard's law is used. The calculated elastic energy is compared with the 1NN, 2NN, and 3NN chemical bond energies to show that elastic energy value is significant for contributing to total energy and thus needs to be considered in Co-Al substitutional solid solution.

2.3 Effects of Ordering: Disordered and Ordered Substitutional Solid Solutions

Supersaturated β-CoAl substitutional solid solution tends to develop B2 ordering of various degrees, depending on solution treatment and quenching [8]. The atomic ordering may be accompanied by a spontaneous lattice strain, which will be investigated. The

ordered phases of β-CoAl in the range of $0.25 \leq x \leq 0.5$ are DO_3 at x=0.25, B2 at x=0.5 and B32 at x=0.5. Equilibrium lattice parameters of ordered phases are different from disordered phases. At the same composition ordered phase lattice parameters are compared with disordered phases i.e., at x=0.25 and x=0.5. The effect of change in the number of 1NN atomic bonds on the lattice parameter due to ordering is investigated.

For x=2/54 in $Co_{1-x}Al_x$, using 3*3*3 supercell the equilibrium lattice parameters are calculated for different Al atoms positions, namely, 1NN, 2NN, and 3NN. The difference in equilibrium lattice parameters for different aluminum atom positions is investigated.

3 Methodology

3.1 Mean-Field Theory of Substitutional Solid Solution $Co_{1-x}Al_x$ for Chemical Energy

The molar free energy of $Co_{1-x}Al_x$, treated as a regular substitutional solid solution [31] is:

Eq. 3.1 $$F = E - TS$$

Where the energy of mixing is given by:

Eq. 3.2 $$E = N_A z \Omega x (1-x)$$

The entropy of mixing is:

Eq. 3.3 $$S = -R\left[x \ln x + (1-x)\ln(1-x)\right]$$

In the above equations, N_A is Avogadro's number, z is the number of bonds per atom, **Ω** is 1NN chemical ordering energy which is given by Eq. 2.1, R is the gas constant, and T is the absolute temperature.

The energy in Eq. 3.2 is the chemical energy that usually considers the 1NN bonds only. For the BCC host lattice of Co-rich β-CoAl alloys, there are 8 1NN bonds per atom, i.e., z=8. In such a situation, **Ω** and $E_{Co\text{-}Al}$ are defined for the 1NN bonds. When energies of the 2NN and 3NN bonds are comparable in magnitude to that of the 1NN bonds, they cannot be neglected and need to be considered.

Consideration of the 2NN bonds contributes a chemical energy term to the total energy:

Eq. 3.4 $$E' = N_A z' \Omega' x(1-x)$$

Where z' = 6, it is the number of 2NN bonds per atom, Ω' is 2NN chemical ordering energy given by Eq. 2.2.

Similarly, consideration of the 3NN bonds contributes a chemical energy term to the total energy:

Eq. 3.5 $$E'' = N_A z'' \Omega'' x(1-x)$$

Where z" =12, it is the number of 3NN bonds per atom, Ω" is 3NN chemical ordering energy given by Eq. 2.3.

3.2 Vegard's Law

For Co-Al BCC-based solid solution, atomistic modeling of 2*2*2 supercell which consists of 8-unit cells is performed using VASP. For a 2*2*2 BCC-based supercell there are 16 atomic positions to define to run simulations, so by specifying Co and Al atoms in these 16 atomic positions the composition of the element in alloy is determined. For pure Co, all the atomic positions are assigned to only Cobalt. For Vegard's law, the composition of Al(x) (in mole fraction) is varied from x=0.25 to 0.5. The compositions considered for simulation are x=0.25, 0.3125, 0.4375, and 0.5. For these Al compositions, the lattice parameters are calculated and fitted against Al composition(x). For x=0.25 among 16 atom positions, 4 atoms out of the 16 are Al atoms and for this composition

four lattice parameters, one ordered phase DO_3 and three disordered A2 phases are calculated. In 2*2*2 supercell the alloy with composition x=4/16=0.25 in $Co_{1-x}Al_x$ is notated as $Co_{12}Al_4$. This is also extended for other compositions as well which indicates that 4 aluminum atoms and 12 cobalt atoms are present in the 2*2*2 BCC supercell.

Similarly, for different Al compositions x=0.3125=5/16, x=0.375=6/16, and x= 0.4375=7/16, four lattice parameters for disordered A2 phase at each composition are calculated. The specific number of Al atoms that are needed to be defined in the total of 16 atomic positions is specified alongside the composition above i.e., for 5/16, 5 out of 16 atoms are Al for x=0.3125. No ordered phase is considered for these off-stoichiometric compositions.

For x=0.5=8/16 two ordered phases, B2 and B32 are considered, whose lattice parameters are calculated along with two disordered phases. All the phases considered, namely, disordered A2, and ordered, DO_3, B2, and B32 are shown in Fig. 3.1.

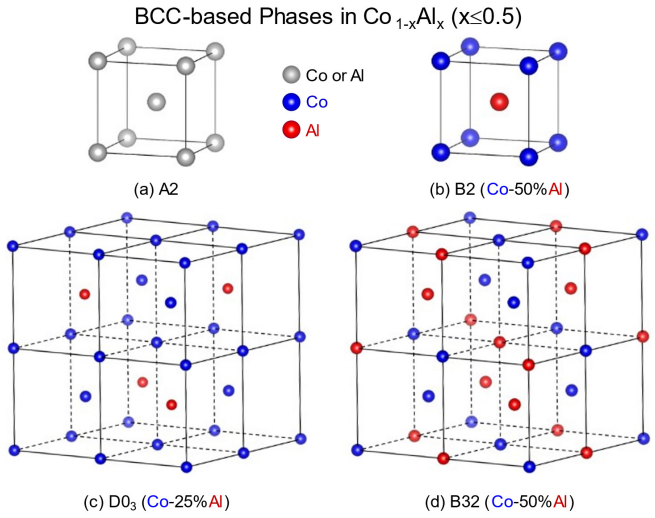

Figure 3.1. Atomic positions of Co and Al in ordered phases of $Co_{1-x}Al_x$

The equilibrium lattice parameters of disordered solid solutions are calculated using the supercell method, considering multiple random atomic configurations at each Al composition within the range $0.25 \leq x \leq 0.5$, and their average values are taken as the lattice parameter at each composition, which improves the statistics and reduces errors. In these simulations, two structural optimization schemes are employed and the results are compared. In one scheme, the atomic positions (i.e., fractional coordinates) in the supercells are fixed. In another scheme, the atoms are allowed to deviate from their ideal positions during structural relaxation. This is done by setting the INCAR control parameters of VASP. Lattice parameters calculated from both schemes are plotted against Al composition.

3.3 Microelasticity Theory

Due to the atomic radius misfit between the solvent Co and solute Al atoms in supersaturated β-CoAl substitutional solid solution, atomic displacements develop in the solid solution, leading to lattice distortion and strain. With Co-host lattice as a reference state, the macroscopic average strain, which is the homogeneous part of the total lattice strain, is given by the theory of micro-elasticity [28]:

Eq. 3.6
$$\bar{\varepsilon} = \frac{a - a_{Co}}{a_{Co}} = \varepsilon_0 x$$

In the above equation, a is the lattice parameter of the solid solution $Co_{1-x}Al_x$ at composition x, a_{Co} is the lattice parameter of Co-host lattice, ε_0 is misfit strain, the equation calculates the total lattice strain induced in the alloy due to change in lattice parameter of substitutional solid solution. The total lattice strain is also expressed in terms of misfit strain and Al atom composition (x).

Whereas the misfit strain is defined in terms of the atomic radii of solvent and solute as shown below.

Eq. 3.7
$$\varepsilon_0 = \frac{r_{Al} - r_{Co}}{r_{Co}}$$

r_{Co} and r_{Al} are the atomic radii of Co and Al, respectively.

It is worth noting that Eq. 3.6 is equivalent to Vegard's law, the linear relationship between the lattice parameter and the composition of solute atoms (x) is defined as:

Eq. 3.8
$$a = a_{Co}(1 + \varepsilon_0 x)$$

The linear plot equation can be deduced from Vegard's law plotted for $Co_{1-x}Al_x$. The equation of the linear plot is expressed as Eq. (3.8) and the corresponding values are found. Eq. (3.6) allows the determination of the misfit strain (and atomic radius misfit) through the composition-dependent lattice parameter data:

Eq. 3.9 $$\varepsilon_0 = \frac{1}{a_{Co}} \frac{da}{dx}$$

From Vegard's law linear plot equation, misfit strain is determined as shown in the above equation by using the lattice parameter $a_{Co} = a(x = 0)$ and the derivative, da/dx which are respectively the intercept and slope of the fitted straight line.

According to the theory of microelasticity [28], the lattice strain caused by atomic radius misfit contributes an elastic energy to the total energy. The elastic energy is calculated from the below equation

Eq. 3.10 $$E''' = N_A V \left(\frac{3(1-2\nu)}{1-\nu}\right) K \varepsilon_0^2 x(1-x)$$

where V is the volume per atom, and K and ν are the bulk modulus and Poisson's ratio, respectively.

E''' is the elastic energy due to atomic radius misfit, and N_A is Avogadro's number.

The bulk modulus (K) of $Co_{1-x}Al_x$ solid solution is calculated for ordered phases DO_3, B2, and B32 by fitting the Energy (E) vs V (volume of supercell) values using 2*2*2 supercell VASP simulations. From the parabolic E vs V data fitting, Bulk modulus is calculated from the equation below for each phase:

Eq. 3.11 $$K = V * d^2E/dV^2$$

Bulk modulus(K) calculated for three ordered phases are plotted against Al Composition(x). And typical value for Bulk modulus and Poisson's ratio are taken for elastic energy (E''') calculation. The Calculated elastic energy is compared with chemical bond energies.

3.4 First-Principles Density Functional Theory

The Density Functional Theory (DFT) solves the many-electron wave function with a simpler single-electron density as the main variable. Hohenberg-Kohn-Sham theory [32] [33] implies that the total energy of a system can be expressed solely in terms of electron density. The physical properties of a system can be found if the electron density is known. DFT-based calculations mainly consider outer electrons only as the inner electron's role in bonding is minimal and they also screen the nuclear core effect partially [34]. By energy minimization, the calculation of a wide range of properties such as structural, chemical, elastic, and thermodynamic properties is enabled by DFT [35]. In this particular study to find out the chemical and elastic energy of β-CoAl, DFT calculations are performed. The First Principles study within the framework of DFT is used to perform total energy calculations. Vienna ab initio simulation package (VASP) code [36] implements the projector-augmented-wave (PAW) method [37]. The generalized gradient approximation (GGA) in the form Perdew-Burke Ernzerhof (PBE) is considered for the exchange-correlation energy [38].

VASP calibration is done using 3*3*3 supercell and 2*2*2 supercell for minimum total energy value to find out the optimum values of plane wave cut-off energy and k-points Monkhorst-pack mesh [39] in the Brillouin zone. The Optimum values of cut-off energy and k-points are 500 eV and 4*4*4 for 3*3*3 supercell respectively. And for 2*2*2 supercell cut of energy is 500 eV and k-points are 5*5*5. Other VASP input parameters used were sufficient leading to well converged total energy.

4 Results and Discussion

4.1 Calculation of Lattice Parameter and Elastic Modulus

4.1.1 Lattice Parameter Calculation using DFT

The equilibrium lattice parameter for the 2*2*2 DO_3 ordered structure of BCC $Co_{1-x}Al_x$ at x=0.25 is calculated by performing VASP simulations. M.J. Mehl et al. [40] calculated the equilibrium lattice parameter of Co-Al BCC unit cell B2 phase using DFT as a=2.862 A^0. Using this value as a reference, total energy calculations at the lattice constant 2a=5.724, for 2*2*2 supercell are simulated. As the Aluminum composition for DO_3 is less than the B2 phase composition the lattice parameter of the DO_3 phase would be less than the B2 phase. So VASP simulations for total energy are performed considering lattice constants 2a<5.724. The energy values would first decrease and then increase indicating energy convergence. The lattice parameter which gives the lowest total energy value is noted and now the simulations using the lattice parameters greater and lower than the noted lattice parameter are performed. Total energy values simulated are plotted against the lattice parameters considered for simulations, the plot follows a parabolic path. Solving the parabolic equation for minimal energy, the equilibrium lattice parameter of the DO_3 structure is found. Fig. 4.1 shows the parabolic plot of energy against the lattice parameter for the β-CoAl DO_3 phase. The lattice parameter units in this entire study are Angstrom's (A^0) and the units of energy are eV.

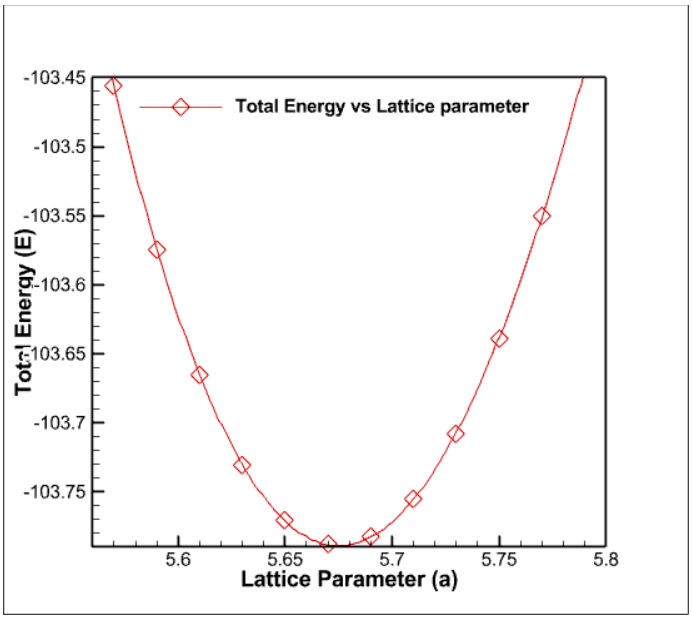

Figure 4.1 Parabolic plot of total energy against lattice parameter for DO_3 phase of β-CoAl

From the above plot, the parabolic equation relating Energy (E) and lattice parameter (a) is given as

Eq. 4.1 $$E = 28.461a^2 - 323.17a + 813.59$$

Phase stability is defined by minimum total energy. For energy dependent on lattice parameters, the equilibrium lattice parameter is that lattice constant which gives minimum energy. The minimum energy condition is first order derivative is zero i.e., dE/da=0.

For minimum energy, the equilibrium lattice constant for the DO_3 phase of β-CoAl is $2a^0$ = 5.677418 A^0, a^0 = 2.838709 A^0, and a^0 is the equilibrium lattice parameter.

Similarly using 2*2*2 supercell for all compositions of Al considered in this study $0.25 \leq x \leq 0.5$ equilibrium lattice parameters for $Co_{1-x}Al_x$ BCC structure unit cell are calculated. At each composition four atomic configurations are considered, ordered, and disordered. Two schemes of operations fixed and relaxed are considered in total energy simulations. All the equilibrium lattice parameters calculated for different atomic configurations at each composition are tabulated from Table 4.1 to 4.5. Lattice parameters calculated using both fixed and relaxed atom schemes are mentioned.

Table 4.1 Equilibrium lattice parameters for x = 0.25 in $Co_{1-x}Al_x$ BCC solid solution

Atomic Arrangement	**Lattice parameter (fixed) A^0**	**Lattice Parameter (relaxed) A^0**
DO_3	2.838709	2.838709
Disordered 1	2.83832815	2.83873959
Disordered 2	2.85217	2.851537
Disordered 3	2.85407	2.85422189

Table 4.2 Equilibrium lattice parameters for x = 0.3125 in $Co_{1-x}Al_x$ BCC solid solution

Atomic Arrangement	**Lattice parameter (fixed) A^0**	**Lattice Parameter (relaxed) A^0**
Disordered 1	2.86156212	2.86043
Disordered 2	2.843831237	2.8442884
Disordered 3	2.86776765	2.86805
Disordered 4	2.866151	2.86776

Table 4.3 Equilibrium lattice parameters for x = 0.375 in $Co_{1-x}Al_x$ BCC solid solution

Atomic Arrangement	Lattice parameter (fixed) A^0	Lattice Parameter (relaxed) A^0
Disordered 1	2.87648613	2.876486129
Disordered 2	2.8836624	2.882545023
Disordered 3	2.869141076	2.86567
Disordered 4	2.88131	2.8818

Table 4.4 Equilibrium lattice parameters for x = 0.4375 in $Co_{1-x}Al_x$ BCC solid solution

Atomic Arrangement	Lattice parameter (fixed) A^0	Lattice Parameter (relaxed) A^0
Disordered 1	2.897636	2.898143832
Disordered 2	2.902956	2.900666
Disordered 3	2.877054642	2.87806778
Disordered 4	2.89110729	2.893031633

Table 4.5 Equilibrium lattice parameters for x=0.5 in $Co_{1-x}Al_x$ BCC solid solution

Atomic Arrangement	Lattice parameter (fixed) A^0	Lattice Parameter (relaxed) A^0
B2	2.85390327	2.853903268
B32	2.908518125	2.908518125
Disordered 1	2.908518125	2.908518125
Disordered 2	2.9146184	2.917785163

Tabulated lattice parameters are fitted against aluminum composition for checking Vegard's law, atomic radius misfit between Co and Al atoms, and for calculating misfit strain. The lattice parameter for pure Co using 2*2*2 supercell is 2.813, as BCC lattice for pure Co is unphysical it is used for comparison only.

4.1.2 Elastic Modulus Calculation of Ordered Phases in β-CoAl Solid Solution

The lattice parameters against which the total energy is fitted for a parabolic plot in the previous chapter are used to find the volume of the 2*2*2 supercell. For calculating the elastic modulus total energy is plotted against the volume of the supercell. Energy (E) against supercell volume (V) is also parabolic. The parabolic plot DO_3 phase of β-CoAl is shown in Fig. 4.2

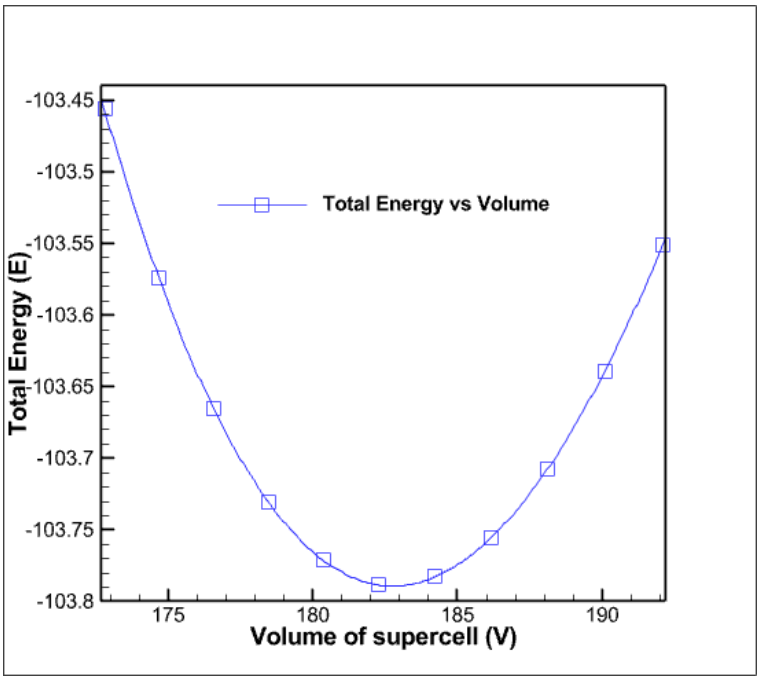

Figure 4.2 Parabolic plot of energy against supercell volume of DO_3 phase

From the above parabolic plot, the energy equation is

Eq. 4.2 $$E = 0.0031V^2 - 1.1222V - 1.0417$$

By using Eq. 3.11 $K = V * d^2E/dV^2$, Bulk modulus or Elastic modulus for the DO_3 phase is calculated. V in the formula is the volume calculated from the equilibrium lattice parameter of the DO_3 phase, $V = (2 * 2.838709)^3$. The value of K= 181 GPa.

Similarly elastic modulus (K) is calculated for pure Co, B2, and B32 phases as 217 GPa, 178 GPa, and 151 GPa, and the values are plotted against aluminum composition.

4.2 Calculation of Chemical Bond Energies

4.2.1 Chemical Bond Energies in BCC $Co_{52}Al_2$

In the 3*3*3 supercell BCC structure of $Co_{1-x}Al_x$ solid solution 54 atomic positions are to be defined for VASP simulation and x=2/54 indicates that 2 aluminum atoms are present in the supercell and the remaining 52 atomic positions are occupied by cobalt atoms, hence x=2/54 in $Co_{1-x}Al_x$ is notated as $Co_{52}Al_2$. In nearest neighbor calculations minimum of two solute atom interactions is required which is why the composition x=2/54 is considered. Firstly, for x = 2/54 = 0.037 i.e., $Co_{52}Al_2$ 1NN, 2NN, and 3NN chemical bond energies are calculated. In this composition, 2 Co atoms are replaced by 2 Al atoms in a pure Co BCC supercell. For 1NN interaction Al atoms in (1/3,1/3,1/3) and (1/6,1/6,1/6) atomic positions are considered remaining all other atomic positions are Co atoms. For 2NN interaction Al atoms in (1/6,1/6,1/6) and (1/6,1/6,1/2) atomic positions are considered. Atomic positions (1/6,1/6,1/6) and (1/6,1/2,1/2) are considered for 3NN Al atoms interaction. In each case, the chemical bond energy of the two atoms considered is calculated by the bond counting method. For the two atomic positions considered in

1NN, 2NN, and 3NN, respective chemical bond energies in pure $Co_{54}Al_0$ and in $Co_{53}Al_1$ are also calculated by the bond counting method. By solving the energy equations calculated for the five cases shown Ω, Ω', Ω'' are calculated. Fig. 4.3 shows the five cases considered for the bond energy calculation.

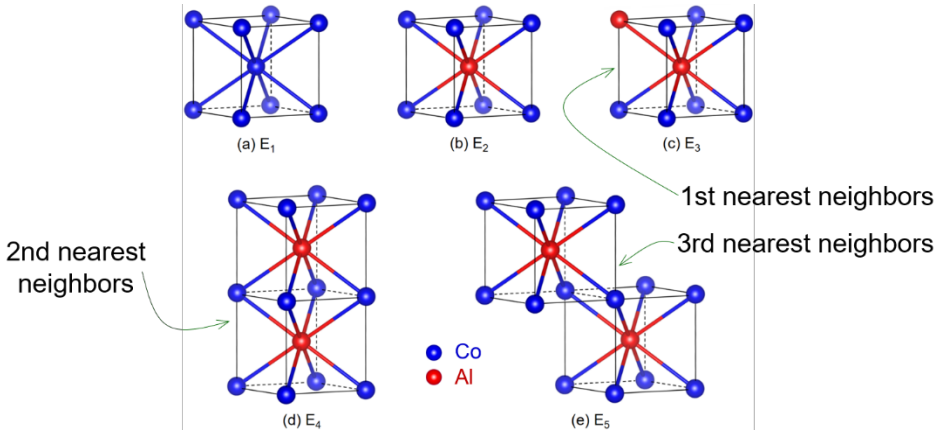

Figure 4.3. Atomic configurations for calculation of 1NN, 2NN, and 3NN chemical bond energies. Only affected atoms in the supercell are shown.

E_1 is the chemical bond energy corresponding to pure Co i.e., $Co_{54}Al_0$. For calculating 1NN interchange bond energies, E_1 is calculated by considering Co atoms in atomic positions (1/6,1/6,1/6) and (1/3,1/3,1/3). For 2NN bond energy calculations (1/6,1/6,1/6) and (1/6,1/6,1/2) atomic position Co atoms are considered. And atomic positions (1/6,1/6,1/6) and (1/6,1/2,1/2) are considered for 3NN energy calculations.

For 1NN bond energy calculation, E_1 corresponding to (1/6,1/6,1/6) from bond counting method is:

Eq. 4.3 $$E_1\left(\frac{1}{6},\frac{1}{6},\frac{1}{6}\right) = 8E_{Co-Co} + 6E'_{Co-Co} + 12E''_{Co-Co}$$

For 1NN bond energy calculation, E_1 corresponding to (1/3,1/3,1/3) is:

Eq. 4.4 $$E_1\left(\frac{1}{3},\frac{1}{3},\frac{1}{3}\right) = 7E_{Co-Co} + 6E'_{Co-Co} + 12E''_{Co-Co}$$

From the above two equations, it can be noted that there are 8 first nearest neighbor bonds, 6 second nearest neighbor bonds, and 12 third nearest bonds in BCC 3*3*3 supercell. These are the same for 2*2*2 BCC supercell also.

So E_1 value for both atoms combined is given by adding Eq. 4.3 and Eq. 4.4

Eq. 4.5 $$E_1 = 15E_{Co-Co} + 12E'_{Co-Co} + 24E''_{Co-Co}$$

E_1 is the chemical bond energy of Co_{54} corresponding to 1NN, $E_{Co\text{-}Co}$ is Co-Co atom bond energy in first nearest neighbor interaction, $E'_{Co\text{-}Co}$ is Co-Co atom bond energy in second nearest neighbor interaction, $E''_{Co\text{-}Co}$ is bond energy between Co-Co atom which are positioned in third nearest neighboring positions.

Calculation of chemical bond energy for 2NN interaction in pure Co BCC 3*3*3 supercell $Co_{54}Al_0$. The atomic positions to be considered are (1/6,1/6,1/6) and

(1/6,1/6,1/2). The chemical bond energy calculation in $Co_{54}Al_0$ for 2NN interaction is denoted by E'_1.

Chemical bond energy considering atom in atomic position (1/6,1/6,1/6) in $Co_{54}Al_0$ for 2NN interaction is given by

Eq. 4.6 $$E_1'\left(\frac{1}{6},\frac{1}{6},\frac{1}{6}\right) = 8E_{Co-Co} + 6E'_{Co-Co} + 12E''_{Co-Co}$$

Chemical bond energy considering atom in atomic position (1/6,1/6,1/2) in $Co_{54}Al_0$ for 2NN interaction is given by

Eq. 4.7 $$E_1'\left(\frac{1}{6},\frac{1}{6},\frac{1}{2}\right) = 8E_{Co-Co} + 5E'_{Co-Co} + 12E''_{Co-Co}$$

The total chemical bond energy of BCC $Co_{50}Al_0$ considering (1/6,1/6,1/6) and (1/6,1/6,1/2) atomic position atoms given by adding Eq. 4.6 and Eq. 4.7.

Eq. 4.8 $$E_1' = 16E_{Co-Co} + 11E'_{Co-Co} + 24E''_{Co-Co}$$

For calculating chemical bond energies at a composition only two atoms are considered as bond energy associated with other atoms cancel out while calculating the difference.

Now for $Co_{54}Al_0$ chemical bond energy considering atomic positions (1/6,1/6,1/6) and (1/6,1/2,1/2) is calculated for 3NN interaction. The energy is denoted by E''_1.

The chemical energy of $Co_{54}Al_0$ considering atom in (1/6,1/6,1/6) atomic position which will be used for 3NN chemical ordering energy calculation is given by

Eq. 4.9 $$E_1''\left(\frac{1}{6},\frac{1}{6},\frac{1}{6}\right) = 8E_{Co-Co} + 6E'_{Co-Co} + 12E''_{Co-Co}$$

Similarly for atom in the (1/6,1/2,1/2) position is given by

Eq. 4.10 $$E_1''\left(\frac{1}{6},\frac{1}{2},\frac{1}{2}\right) = 8E_{Co-Co} + 6E'_{Co-Co} + 11E''_{Co-Co}$$

Chemical energy value of $Co_{54}Al_0$ considering positions (1/6,1/6,1/6) and (1/6,1/2,1/2) is given by

Eq. 4.11 $$E_1'' = 16E_{Co-Co} + 12E'_{Co-Co} + 23E''_{Co-Co}$$

E_1, E'_1, and E''_1 are the same $E_1=E'_1=E''_1$ for $Co_{54}Al_0$ which is the total energy value of $Co_{54}Al_0$ calculated from VASP simulation using extrapolated lattice parameter, but are represented differently E_1 in terms of 1NN atoms, E'_1 in terms of 2NN atoms and E''_1 in terms of 3NN atoms. This is done for the simplification of **Ω**, **Ω'**, **Ω''** calculations. While calculations of **Ω** chemical bonds corresponding to those atoms other than (1/6,1/6,1/6) and (1/3,1/3,1/3) cancel out. For 2NN and

3NN energy calculations also the chemical bonds of atoms other than those considered cancel out.

Similarly, for $Co_{53}Al_1$ chemical bond energy E_2 is calculated by considering atoms in atomic positions (1/6,1/6,1/6) and (1/3,1/3,1/3) which will be used of 1NN chemical energy, atomic positions (1/6,1/6,1/6) and (1/6,1/6,1/2) for 2NN energy calculation (E_2') and atomic positions (1/6,1/6,1/6) and (1/6,1/2,1/2) for 3NN energy calculation (E_2''). Atomic position (1/6,1/6,1/6) is occupied by Al atom in $Co_{53}Al_1$.

Chemical bond energy (E_2) of $Co_{53}Al_1$ considering atomic positions (1/6,1/6,1/6) and (1/3,1/3,1/3) which are used for calculating 1NN energies is given by

Eq. 4.12 $$E_2 = 8E_{Co-Al} + 7E_{Co-Co} + 6E'_{Co-Al} + 6E'_{Co-Co} + 12E''_{Co-Al} + 12E''_{Co-Co}$$

$E_{Co\text{-}Al}$ is the bond energy between Co and Al atoms in the first nearest neighbor position, $E'_{Co\text{-}Al}$ is the bond energy between Co and Al atoms in the second nearest neighbor position and $E''_{Co\text{-}Al}$ is the bond energy between Co and Al atoms in the third nearest neighbor position.

Chemical bond energy (E'_2) of $Co_{53}Al_1$ considering atomic positions (1/6,1/6,1/6) and (1/6,1/6,1/2) which are used for 2NN energy calculations is given by

Eq. 4.13 $$E_2' = 8E_{Co-Al} + 8E_{Co-Co} + 6E'_{Co-Al} + 5E'_{Co-Co} + 12E''_{Co-Al} + 12E''_{Co-Co}$$

Chemical bond energy (E''$_2$) of $Co_{52}Al_2$ considering atomic positions (1/6,1/6,1/6) and (1/6,1/2,1/2) which are used for 3NN energy calculations is given by

Eq. 4.14 $$E''_2 = 8E_{Co-Al} + 8E_{Co-Al} + 6E'_{Co-Al} + 6E'_{Co-Co} + 12E''_{Co-Al} + 11E''_{Co-Co}$$

Similar to Co_{54}, in $Co_{53}Al_1$ $E_2 = E'_2 = E''_2$, but are represented differently.

For $Co_{52}Al_2$, Chemical bond energy (E_3) considering the two Al atoms in atomic positions (1/6,1/6,1/6) and (1/3,1/3,1/3) which are in 1NN positions is given by

Eq.4.15 $$E_3 = E_{Al-Al} + 14E_{Co-Al} + 12E'_{Co-Al} + 24E''_{Co-Al}$$

E_3 is the total energy of $Co_{52}Al_2$ for Al atoms occupying 1NN positions. The above equation doesn't represent the chemical energy for all the atoms in the supercell but only for (1/6,1/6,1/6) and (1/3,1/3,1/3) as chemical bond energy for other atoms cancels out while calculating '**Ω**'.

For $Co_{52}Al_2$, Al atoms occupying 2NN positions (1/6,1/6,1/6) and (1/6,1/6,1/2) chemical bond energy (E_4) is given by

Eq. 4.16 $$E_4 = 16E_{Co-Al} + E'_{Al-Al} + 10E'_{Co-Al} + 24E''_{Co-Al}$$

E_4 is the total energy of $Co_{52}Al_2$ consisting of Al atoms in the 2NN position. Eq. 4.16 represents the two Al atom bond energies other atom's bond energy cancels out while calculating **Ω**'.

Chemical bond energy(E_5) in $Co_{52}Al_2$ for the two Al atoms occupying 3NN positions (1/6,1/6,1/6) and (1/6,1/2,1/2) is given by

Eq. 4.17 $$E_5 = 16E_{Co-Al} + 12E'_{Co-Al} + E''_{Al-Al} + 22E''_{Co-Al}$$

E_5 is the total energy of $Co_{52}Al_2$ consisting of Al atoms in 3NN positions. Eq. 4.17 represents bond energy in terms of two Al atoms that are in the 3NN position. While calculating **Ω**'' other atom bond energies cancel out.

The first nearest neighbor chemical ordering energy (**Ω**) in 3*3*3 supercell of BCC Co-Al solid solution $Co_{52}Al_2$ is calculated from Eq. 4.5, Eq. 4.12, and Eq. 4.15, which are equations of E_1, E_2, and E_3. The equation of **Ω** for $Co_{52}Al_2$ in terms of E_1, E_2 and E_3 by the following equation:

Eq. 4.18 $$\Omega = \mathrm{E_{Co-Al}} - \frac{E_{Co-Co}+E_{Al-Al}}{2} = E_2 - \frac{E_1+E_3}{2}$$

The second nearest neighbor chemical ordering energy (Ω') in 3*3*3 supercell of BCC Co-Al solid solution $Co_{52}Al_2$ is calculated From Eq. 4.8, Eq. 4.13, and Eq. 4.16, which are equations of E'_1, E'_2 and E_4. It is already mentioned that $E'_1 = E_1$ and $E'_2 = E_2$, E'_1 and E'_2 equations are expressed in terms of 1NN atoms but the values are the same as that of E_1 and E_2 respectively. The equation of Ω' for $Co_{52}Al_2$ in terms of E_1, E_2, E_4 is given by

Eq. 4.19 $$\Omega' = \mathrm{E}'_{\mathrm{Co-Al}} - \frac{E'_{Co-Co}+E'_{Al-Al}}{2} = E_2 - \frac{E_1+E_4}{2}$$

Ω'' in 3*3*3 supercell of BCC Co-Al solid solution $Co_{52}Al_2$ is calculated from Eq. 4.11, Eq. 4.14, and Eq. 4.17, which are equations of E''_1, E''_2, E_5. $E''_1 = E_1$ and $E''_2 = E_2$. The equation of Ω'' for $Co_{52}Al_2$ in terms of E_1, E_2 and E_5 is given by

Eq. 4.20 $$\Omega'' = \mathrm{E}''_{\mathrm{Co-Al}} - \frac{E''_{Co-Co}+E''_{Al-Al}}{2} = E_2 - \frac{E_1+E_5}{2}$$

Equations for Ω, Ω' Ω'' for x=2/54 in $Co_{1-x}Al_x$ in terms of the total energy values of Co_{54} (E_1), $Co_{53}Al_1$ (E_2), $Co_{52}Al_2$ 1NN (E_3), $Co_{52}Al_2$ 2NN energy(E_4) and $Co_{52}Al_2$(E_5). E_1, E_2, E_3, E_4, and E_5 are VASP simulation outputs of 3*3*3 supercell corresponding to the Al atom position shown in Figure 4.3.

4.2.2 Chemical Bond Energies in $Co_{50}Al_4$

For x=4/54 =0.074 in $Co_{1-x}Al_x$ BCC structure 1NN, 2NN, and 3NN chemical bond energy Ω, Ω' and Ω'' are calculated for $Co_{50}Al_4$ i.e., 4 Al atoms in a cluster of Co atoms in 3*3*3 supercell BCC structure in the similar way done for $Co_{52}Al_2$. Extrapolated unit cell lattice parameter from Vegard's plot is used for the simulations. For $Co_{50}Al_4$ the atomic arrangements and their corresponding energies for the calculation of 'Ω' are given in Figure 4.4.

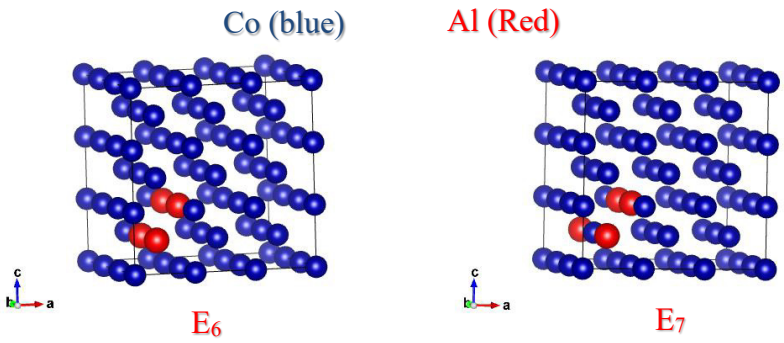

Figure 4.4 Two atomic configurations of $Co_{50}Al_4$ which are used for 'Ω' Calculations. (Co atoms are depicted in Blue and Al atoms in red. Visualization is done using VESTA)

E_6 is the energy of $Co_{50}Al_4$ in which Al atomic positions are (1/6,1/6,1/6), (1/3,2/3,1/3), (1/3,1/3,1/3) and (1/6,1/2,1/6). E_7 is the energy of $Co_{50}Al_4$ in which Al atomic positions are (1/6,1/6,1/6), (1/3,2/3,1/3), (1/3,1/3,1/3) and (1/6,5/6,1/6). E_6 and E_7 values are calculated from VASP simulations for the atomic configuration shown in Fig. 4.4.

The difference between E_6 and E_7 atomic configurations is that the Al atom (1/6,1/2,1/6) in E_6 is exchanged with the Co atom (1/6,5/6,1/6) in E_7. E_6 and E_7 energies of $Co_{50}Al_4$ are expressed in terms of bond energies of two atoms in (1/6,1/2,1/6) and (1/6,5/6,1/6) positions. Bond energies of remaining atoms that are not in (1/6,1/2,1/6) and (1/6.5/6,1/6) positions are equal for E_6 and E_7.

The E_6 energy equation considering the aluminum atom in (1/6,1/2,1/6) and the cobalt atom in (1/6,5/6,1/6) is given by

Eq. 4.21 $$E_6 = 2E_{Al-Al} + 7E_{Co-Al} + 7E_{Co-Co} + E'_{Al-Al} + 6E'_{Co-Al} + 4E'_{Co-Co} + 12E''_{Co-Al} + 12E''_{Co-Co}$$

The E_7 energy equation for considered atoms is given by

Eq. 4.22 $$E_7 = E_{Al-Al} + 9E_{Co-Al} + 6E_{Co-Co} + E'_{Al-Al} + 6E'_{Co-Al} + 4E'_{Co-Co} + 12E''_{Co-Al} + 12E''_{Co-Co}$$

The difference between Eq. 4.22 and Eq. 4.21 gives

Eq. 4.23 $$E_7 - E_6 = 2\Omega$$

Total energy (E_8) of $Co_{50}Al_4$ consisting of aluminum atoms in atomic positions (1/6,1/6,1/6), (1/3,1/3,1/3), (1/3,2/3,1/3) and (1/6,1/2,1/2) is calculated from VASP simulations. The atomic configuration of E_8 is shown in Figure 4.5.

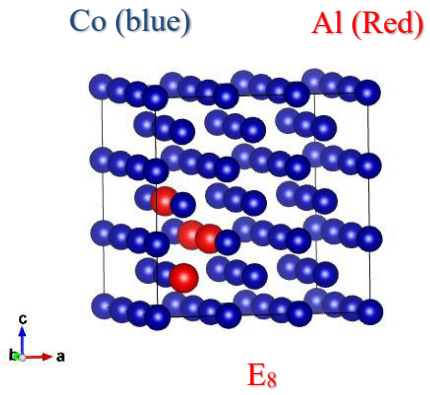

Figure 4.5 $Co_{50}Al_4$ (E_8) atomic configuration with Al positions at (1/6,1/6,1/6), (1/3,1/3,1/3), (1/3,2/3,1/3) and (1/6,1/2,1/2)

Atomic positions that need to be considered by comparing E_8 and E_6 are (1/6,1/2,1/6) and (1/6,1/2,1/2). All other atom's bond energies are the same in both configurations.

E_6 in terms of (1/6,1/2,1/6) and (1/6,1/2,1/2) atomic positions atoms expressed by

Eq. 4.24 $$E_6 = 6E_{Co-Co} + 8E_{Co-Al} + 2E_{Al-Al} + 5E'_{Co-Co} + 5E'_{Co-Al} + E'_{Al-Al} + 11E''_{Co-Co} + 13E''_{Co-Al}$$

E_8 in terms of (1/6,1/2,1/6) and (1/6,1/2,1/2) atomic positions atoms expressed by

Eq. 4.25 $E_8 = 6E_{Co-Co} + 8E_{Co-Al} + 2E_{Al-Al} + 4E'_{Co-Co} + 7E'_{Co-Al} + 12E''_{Co-Co} + 11E''_{Co-Al} + E''_{Al-Al}$

Calculating the difference between Eq. 4.25 and Eq. 4.24 gives

Eq. 4.26 $E_8 - E_6 = 2\Omega' - 2\Omega''$

Another atomic configuration for $Co_{50}Al_4$ (E_9) with aluminum atom positions at (1/6,1/6,1/6), (1/3,1/3,1/3), (1/3,2/3,1/3) and (1/6,1/2,5/6) is considered. E_9 is calculated from the VASP simulation performed for this atomic configuration. Figure 4.6 depicts the atomic configuration of E_9.

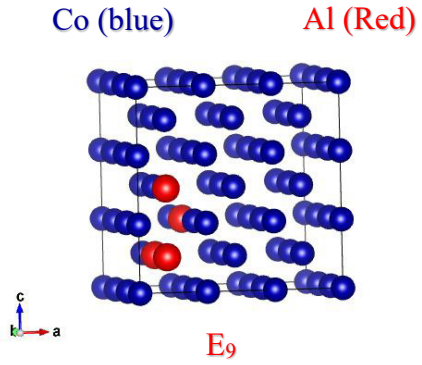

Figure 4.6 $Co_{50}Al_4$ (E_9) atomic configuration with Al positions at (1/6,1/6,1/6), (1/6,1/6,1/2), (1/3,2/3,1/3) and (1/6,1/2,1/6)

The two atomic positions that need to be considered for expressing energies E_6 and E_9 are (1/6,1/6,1/2) and (1/3,1/3,1/3).

E_6 in terms of (1/6,1/6,1/6) and (1/3,1/3,1/3) is given by

Eq. 4.27 $$E_6 = 7E_{Co-Co} + 6E_{Co-Al} + 2E_{Al-Al} + 5E'_{Co-Co} + 6E'_{Co-Al} + E'_{Al-Al} + 11E''_{Co-Co} + 13E''_{Co-Al}$$

E_9 in terms of (1/6,1/6,1/2) and (1/3,1/3,1/3) is given by

Eq. 4.28 $$E_9 = 5E_{Co-Co} + 10E_{Co-Al} + 5E'_{Co-Co} + 6E'_{Co-Al} + E'_{Al-Al} + 12E''_{Co-Co} + 11E''_{Co-Al} + E''_{Al-Al}$$

The mathematical Difference of Eq. 4.28 and Eq. 4.27 gives:

Eq. 4.29 $$E_9 - E_6 = 4\Omega - 2\Omega''$$

Solving Eq. 4.23, Eq. 4.26, and Eq. 4.29 Chemical ordering energy values for 1NN, 2NN, and 3NN (**Ω**, **Ω'**, **Ω''**) are calculated for $Co_{50}Al_4$.

4.2.3 Chemical Bond Energies in $Co_{14}Al_2$

For x=0.125=2/16 in $Co_{1-x}Al_x$ BCC structure chemical bond energies (**Ω**, **Ω'**, **Ω''**) are calculated from total energy values calculated using VASP simulations. Total energies are calculated for 1NN, 2NN, and 3NN aluminum positions in the 2*2*2 supercell of $Co_{14}Al_2$. Figure 4.7 depicts the atomic configurations for $Co_{1-x}Al_x$

2*2*2 supercells with different aluminum compositions. For $Co_{16}Al_0$ total energy is denoted by E_{10}, for $Co_{15}Al_1$ as E_{11}, $Co_{14}Al_2$ with 1NN aluminum atom position as E_{12}, for 2NN aluminum position of $Co_{14}Al_2$ as E_{13} and 3NN aluminum position of $Co_{14}Al_2$ as E_{14}.

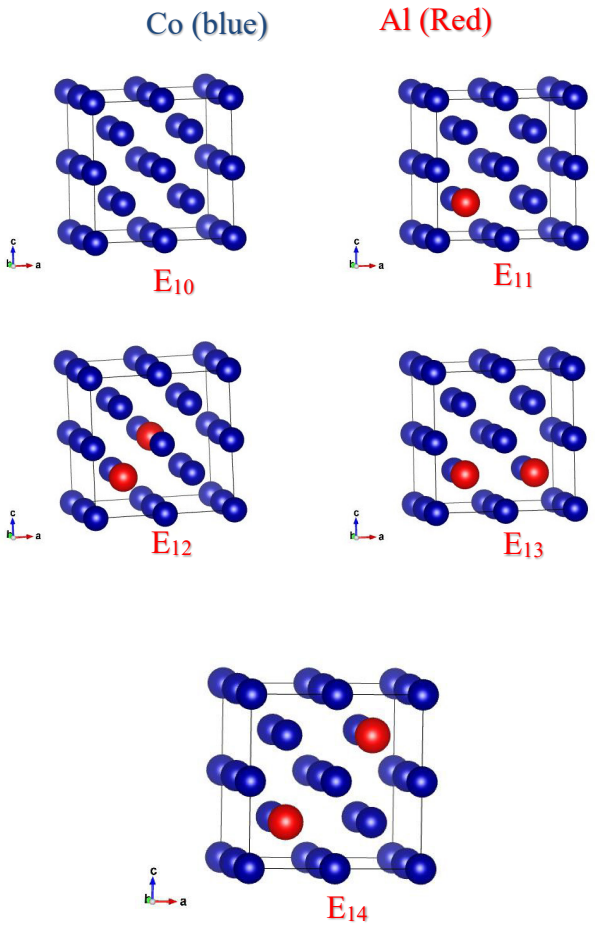

Figure 4.7 Atomic configurations for calculating 1NN, 2NN, and 3NN chemical bond energy for $Co_{14}Al_2$.

Following bond counting, E_{10}, E_{11}, and E_{12} total energies are expressed in terms of (1/4,1/4,1/4) and (1/2,1/2,1/2) position atoms which are 1NN atoms. Energy equations considering 1NN atoms are given in the below equations.

Eq. 4.30 $E_{10} = 15E_{Co-Co} + 12E'_{Co-Co} + 24E''_{Co-Co}$

Eq. 4.31 $E_{11} = 7E_{Co-Co} + 8E_{Co-Al} + 6E'_{Co-Co} + 6E'_{Co-Al} + 12E''_{Co-Co} + 12E''_{Co-Al}$

Eq. 4.32 $E_{12} = 14E_{Co-Al} + E_{Al-Al} + 12E'_{Co-Al} + 24E''_{Co-Al}$

From Eq. 4.30, Eq. 4.31, and Eq. 4.32 1NN chemical ordering energy (Ω) is given by

Eq. 4.33 $\Omega = \mathrm{E}_{11} - \frac{E_{10}+E_{12}}{2}$

E_{10}, E_{11}, and E_{13} total energies expressed in terms of 2NN atoms in (1/4,1/4,1/4) and (3/4,1/2,1/2) positions are given in the below equations.

Eq. 4.34 $E_{10} = 16E_{Co-Co} + 11E'_{Co-Co} + 24E''_{Co-Co}$

Eq. 4.35 $E_{11} = 8E_{Co-Co} + 8E_{Co-Al} + 4E'_{Co-Co} + 7E'_{Co-Al} + 12E''_{Co-Co} + 12E''_{Co-Al}$

Eq. 4.36 $E_{13} = 16E_{Co-Al} + 8E'_{Co-Al} + 3E'_{Al-Al} + 24E''_{Co-Al}$

Comparing Eq. 4.34, Eq. 4.35 and Eq. 4.36 the 2NN chemical ordering energy(Ω') is given by

Eq. 4.37 $3\Omega' = \mathrm{E}_{11} - \frac{E_{10}+E_{13}}{2}$

E_{10}, E_{11}, and E_{14} total energies expressed in terms of 3NN atoms in (1/4,1/4,1/4) and (3/4,1/4,3/4) positions are given by the following equations.

Eq. 4.38 $E_{10} = 16E_{Co-Co} + 12E'_{Co-Co} + 23E''_{Co-Co}$

Eq. 4.39 $E_{11} = 8E_{Co-Co} + 8E_{Co-Al} + 6E'_{Co-Co} + 6E'_{Co-Al} + 15E''_{Co-Al} + 8E''_{C0-C0}$

Eq. 4.40 $E_{14} = 16E_{Co-Al} + 12E'_{Co-Al} + 16E''_{Co-Al} + 7E''_{Al-Al}$

Comparing Eq. 4.38, Eq. 4.39, and Eq. 4.40 3NN chemical bond energy (Ω'') is given by

Eq. 4.41 $7\Omega'' = E_{11} - \frac{E_{10}+E_{14}}{2}$

4.2.4 Chemical bond energies in $Co_{12}Al_4$

For x=0.25 Ω, Ω' and Ω'' are calculated by considering the DO_3 structure 2*2*2 supercell. By interchanging the Co and Al atom positions total energy values are calculated using VASP calculation. 1NN,2NN, and 3NN chemical bond energy values are expressed in terms of the total energy values by the bond counting method. Figure 4.8 shows the atomic configurations of $Co_{12}Al_4$ considered.

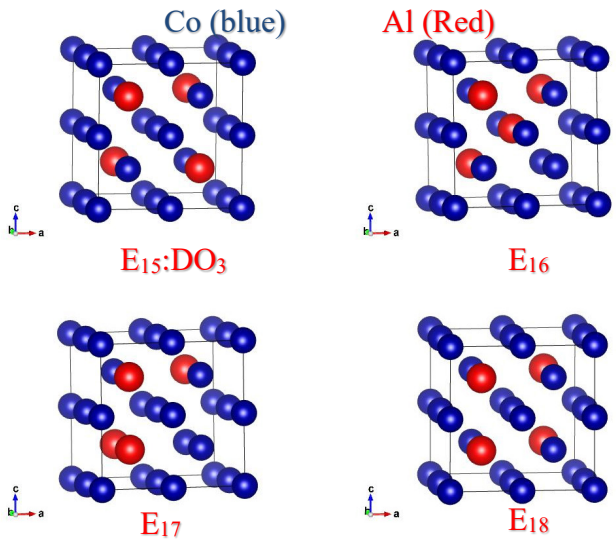

Figure 4.8 Atomic configuration of DO_3

$Co_{12}Al_4$ for different Aluminum atom positions in 2*2*2 supercell.

E_{15}, E_{16}, E_{17}, and E_{18} are total energy calculated from VASP simulation. E_{15} is the energy of the ordered phase DO_3 configuration. The difference between E_{15} and E_{16} is atoms in (1/2,1/2,1/2) and (3/4,1/4,1/4) positions. So E_{15} and E_{16} energies

are expressed in terms of bond energies of the two atoms in atomic positions (1/2,1/2,1/2) and (3/4,1/4,1/4).

E_{15} in terms of bond energies of (1/2,1/2,1/2) and (3/4,1/4,1/4) is given by

Eq. 4.42 $$E_{15} = 11E_{Co-Al} + 4E_{Co-Co} + 6E'_{Co-Al} + 6E'_{Co-Co} + 12E''_{Al-Al} + 12E''_{Co-Co}$$

Eq. 4.43 $$E_{16} = 5E_{Co-Al} + 7E_{Co-Co} + 3E_{Al-Al} + 6E'_{Co-Al} + 6E'_{Co-Co} + 24E''_{Co-Al}$$

Comparing Eq. 4.42 and Eq. 4.43 the difference between E_{16} and E_{15} is

Eq. 4.44 $$E_{16} - E_{15} = -6\Omega + 24\Omega''$$

E_{17} and E_{15} energies are expressed in terms of bond energies of atoms (1/4,1/4,1/4) and (3/4,1/4,1/4). The equations are

Eq. 4.45 $$E_{15} = 8E_{Co-Co} + 8E_{Co-Al} + 11E'_{Co-Al} + 12E''_{Co-Co} + 12E''_{Al-Al}$$

Eq. 4.46 $$E_{17} = 8E_{Co-Co} + 8E_{Co-Al} + 3E'_{Co-Al} + 4E'_{Al-Al} + 4E'_{Co-Co} + 24E''_{Co-Al}$$

The difference between E_{17} and E_{15} from Eq. 4.46 and Eq. 4.45 is

Eq. 4.47 $E_{17} - E_{15} = -8\Omega' + 24\Omega''$

E_{18} and E_{15} energies are expressed in terms of bond energies of 4 atoms in atomic positions (1/4,1/4,1/4), (3/4,1/4,1/4), (1/4,3/4,1/4) and (3/4,3/4,1/4). The energy equations are

Eq. 4.48 $E_{15} = 16E_{Co-Al} + 16E_{Co-Co} + 20E'_{Co-Al} + 23E''_{Co-Co} + 23E''_{Al-Al}$

Eq. 4.49 $E_{18} = 16E_{Co-Al} + 16E_{Co-Co} + 4E'_{Al-Al} + 12E'_{Co-Al} + 4E'_{Co-Co} + 7E''_{Al-Al} + 32E''_{Co-Al} + 7E''_{Co-Co}$

The difference between E_{18} and E_{15} from Eq. 4.48 and Eq. 4.49 is

Eq. 4.50 $E_{18} - E_{15} = -8\Omega' + 32\Omega''$

Solving Eq. 4.44, Eq. 4.47, and Eq. 4.50 the Ω, Ω', Ω'' values for $Co_{12}Al_4$ are calculated.

4.2.5 Chemical Bond Energies in Co_8Al_8

For x=0.5 in $Co_{1-x}Al_x$ 1NN, 2NN, and 3NN chemical bond energies (Ω, Ω', Ω'') are calculated from the total energies of CoAl BCC solid solution for different

aluminum atom positions. Figure 4.9 shows the atomic configuration of the Co_8Al_8 B2 phase for different atom positions in the 2*2*2 supercell.

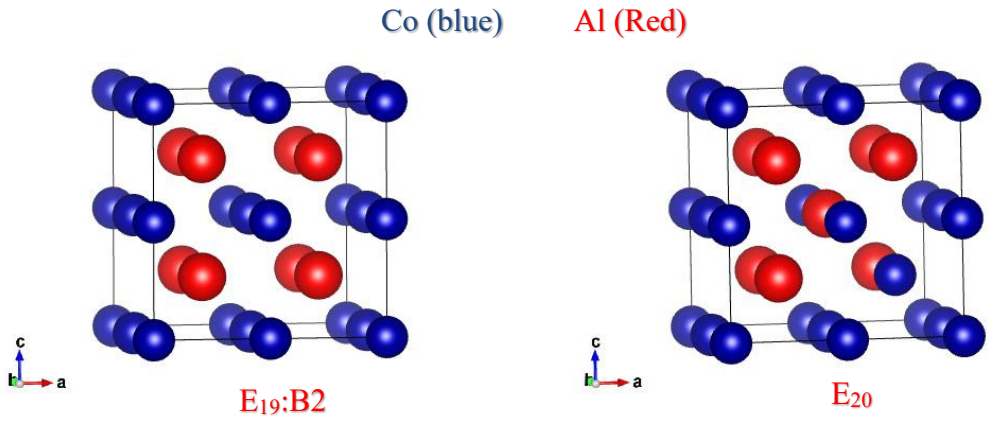

Figure 4.9 Atomic configurations for B2 phase Co_8Al_8 in 2*2*2 supercell

Atomic positions (3/4,1/4,1/4) and (1/2,1/2,1/2) differ in E_{19} and E_{20} configurations. E_{19} and E_{20} total energy values are expressed in terms of bond energies of the two atoms in (3/4,1/4,1/4) and (1/2,1/2,1/2) positions. The equations are

Eq. 4.51 $E_{19} = 15E_{Co-Al} + 6E'_{Al-Al} + 6E'_{Co-Co} + 12E''_{Al-Al} + 12E''_{Co-Co}$

Eq. 4.52 $E_{20} = E_{Co-Al} + 7E_{Co-Co} + 7E_{Al-Al} + 12E'_{Co-Al} + 24E'_{Co-Al}$

Comparing Eq. 4.51 and Eq. 4.52 gives

Eq. 4.53 $E_{20} - E_{19} = -14\Omega + 12\Omega' + 24\Omega''$

Total energies for B32 configurations by interchanging the atom positions are also calculated using VASP simulations of 2*2*2 supercell Co_8Al_8. Figure 4.10 shows the atomic configurations considered for the B32 phase.

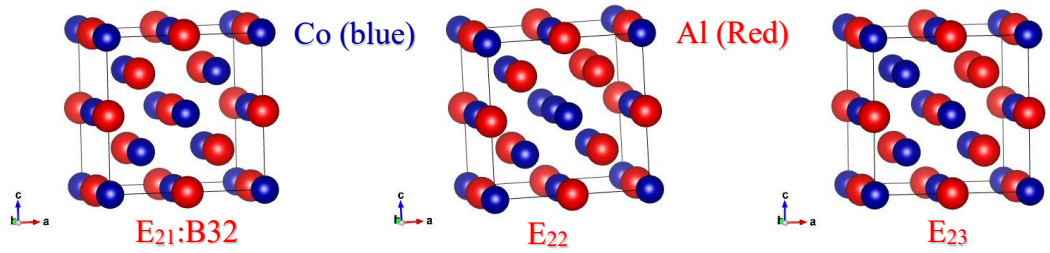

Fig. 4.10 Atomic configurations for B32 phase for different atomic positions in Co_8Al_8 2*2*2 supercell.

Atomic positions which are different in E_{21} and E_{22} atomic configurations are (1/2,1/2,1/2) and (3/4,1/4,3/4). Total energies E_{21} and E_{22} are expressed in terms of the bond energies of these atoms, the equations are given as follows

Eq. 4.54 $$E_{21} = 4E_{Co-Co} + 7E_{Co-Al} + 4E_{Al-Al} + 12E'_{Co-Al} + 12E''_{Co-Co} + 12E''_{Al-Al}$$

Eq. 4.55 $$E_{22} = 3E_{Co-Co} + 9E_{Co-Al} + 3E_{Al-Al} + 6E'_{Co-Co} + 6E'_{Al-Al} + 24E''_{Co-Al}$$

The mathematical difference of Eq. 4.55 and Eq. 4.54 gives

Eq. 4.56 $E_{22} - E_{21} = 2\Omega - 12\Omega' + 24\Omega''$

Atomic positions which are different in E_{21} and E_{23} atomic configurations are (1/4,1/4,3/4) and (3/4,1/4,3/4). The total energies of E_{21} and E_{23} are expressed in terms of the bond energies of these atoms, the equations are given as follows

Eq. 4.57 $E_{21} = 8E_{Co-Al} + 4E_{Co-Co} + 4E_{Al-Al} + 11E'_{Co-Al} + 12E''_{Al-Al} + 12E''_{Co-Co}$

Eq. 4.58 $E_{23} = 8E_{Co-Al} + 4E_{Co-Co} + 4E_{Al-Al} + 3E'_{Co-Al} + 4E'_{Co-Co} + 4E'_{Al-Al} + 24E''_{Co-Al}$

The mathematical difference of Eq. 4.57 and Eq. 4.58 gives

Eq. 4.59 $E_{23} - E_{21} = -8\Omega' + 24\Omega''$

For x=0.5, 1NN, 2NN, and 3NN chemical bond energies are expressed in terms of total energy values of Co_8Al_8 2*2*2 supercell considered for calculations.

In this chapter, equations of 1NN, 2NN, and 3NN chemical bond energies (**Ω**, **Ω**', **Ω**'') for five aluminum compositions (x) 0.037, 0.074, 0.125, 0.25, and 0.5 in BCC $Co_{1-x}Al_x$ are shown.

4.3 Testing the Hypotheses

Following equations 3.1 to 3.5 and 3.10, the molar free energy of $Co_{1-x}Al_x$ is given by:

Eq. 4.60

$$\begin{aligned} F &= E + E' + E'' + E''' - TS \\ &= N_A\left[z\Omega + z'\Omega' + z''\Omega'' + V\frac{3(1-2\nu)}{1-\nu}K\varepsilon_0^2 \right]x(1-x) + RT\left[x\ln x + (1-x)\ln(1-x) \right] \end{aligned}$$

The results will be discussed in terms of the relative importance of individual energy terms in the free energy function. For convenience in result analysis and discussion, the following energy coefficients are defined:

Eq. 4.61

$$c = z\Omega \qquad c' = z'\Omega' \qquad c'' = z''\Omega'' \qquad c''' = V\frac{3(1-2\nu)}{1-\nu}K\varepsilon_0^2$$

In Eq. 4.61, c is the 1NN chemical energy coefficient, c' is the 2NN chemical energy coefficient, c'' is the 3NN chemical energy coefficient and c''' is the elastic energy coefficient.

4.3.1 First nearest neighbor, second nearest neighbor, and third nearest neighbor chemical bond energies

In Chapter 2.1.1, it is proposed to calculate the bond energies of 1NN, 2NN, and 3NN chemical bond energies and compare their values to reveal their respective importance. Such calculations are performed using a 3*3*3 supercell with atomic configurations shown in Fig. 4.3. The energies of the atomic configurations are summarized in Table 4.6.

Table 4.6. The energies of atomic configurations in Fig. 4.3. that are used for calculating 1NN, 2NN and 3NN chemical bond energies in $Co_{52}Al_2$

	E_1	E_2	E_3	E_4	E_5
energy (eV)	-378.084555	-375.697674	-372.972622	-373.401898	-373.398153

Using Eq. 4.18 and calculated energies E_1, E_2, and E_3 given in Table 4.6 for x=2/54 in $Co_{1-x}Al_x$ which is $Co_{52}Al_2$, $\Omega = -0.169$ eV. Using $z = 8$ for 1NN bonds per atom, the 1NN chemical energy coefficient is calculated $c = z\Omega = -1.353$ eV.

Similarly using Eq. 4.19 and calculated energies E_1, E_2, and E_4 in Table 4.6 gives $\Omega' = 0.0456$ eV. Using $z' = 6$ for 2NN bonds per atom, the 2NN chemical energy coefficient is calculated $c' = z'\Omega' = 0.273$ eV.

Using Eq. 4.20 and calculated energies E_1, E_2, and E_5 in Table 4.6 gives $\Omega'' = 0.0437$ eV. Using $z'' = 12$ for 3NN bonds per atom, the 3NN chemical energy coefficient is calculated $c'' = z''\Omega'' = 0.524$ eV.

Table 4.7. Chemical ordering energies of 1NN, 2NN, and 3NN and elastic energy per solute atom.

	Ω	Ω'	Ω''	c'''
energy (eV)	-0.169	0.0456	0.0437	0.175
ratio to $\|\Omega\|$	100%	27.0%	25.9%	103.6%
B2	Yes	Yes	Yes	
DO_3	Yes	No	Yes	
B32	No	No	Yes	

The calculated chemical ordering energies Ω, Ω', and Ω'' are summarized in Table 4.7. These energies are responsible for the development of atomic ordering and potential formation of ordered phases shown in Fig 4.11. Since the 2NN and 3NN bonds contribute 27.0% and 25.9%, respectively, compared to the ordering energy of the 1NN bonds, their values are significant, so the 2NN and 3NN bonds are equally important as the 1NN bonds. In particular, the 1NN ordering energy Ω is dominant in magnitude, its negative value $\Omega < 0$ favors 1NN Co-Al bonds, and is responsible for the B2 ordering and DO_3 ordering but not B32 ordering. The 2NN ordering energy Ω' has a positive value $\Omega' > 0$, it disfavors 2NN Co-Al bonds, and is responsible for the B2 ordering but not DO_3 ordering and B32 ordering. The 3NN ordering energy Ω'' also has a positive value $\Omega'' >$

0, disfavors 3NN Co-Al bonds, and is responsible for B2 ordering, DO_3 ordering and B32 ordering. The effects of the 1NN, 2NN, and 3NN bond energies on the development of atomic ordering are also summarized in Table 4.7, which shows that B2 ordering is favored over DO_3 and B32 ordering.

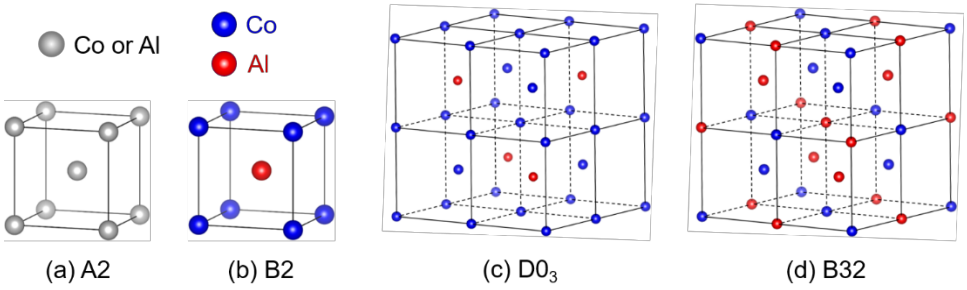

Figure 4.11 Phases potentially formed in β-CoAl substitutional solid solution: (a) disordered A2 $Co_{1-x}Al_x$, (b) ordered B2 $Co_{0.5}Al_{0.5}$, (c) ordered DO_3 $Co_{0.75}Al_{0.25}$, and (d) ordered B32 $Co_{0.5}Al_{0.5}$.

The calculated chemical energy coefficients c, c', and c'' are summarized in Table 4.8. These energy coefficients are responsible for the formation of the disordered A2 phase. In particular, their combined coefficient $c + c' + c''$ defines the free energy of the disordered A2 solid solution. Since 2NN and 3NN bonds contribute 20.2% and 38.7%, respectively, compared to the chemical energy of the 1NN bonds, their values are significant, and the 2NN and 3NN bonds are equally important as the 1NN bonds. Particularly the combined contribution of the 2NN and 3NN bonds accounts for 58.9% compared to 100% of the chemical energy of the 1NN bonds, thus their roles need to be considered.

Table 4.8. Energy coefficients of 1NN, 2NN, 3NN chemical bonds, and atomic radius misfit strain.

	c	c'	c''	c'''	$c'+c''$	$c'+c''+c'''$
energy (eV)	-1.353	0.273	0.524	0.175	0.797	0.972
ratio to $\|c\|$	100%	20.2%	38.7%	12.9%	58.9%	71.8%

4.3.2 Dependence of Chemical Ordering Energy on Alloy Composition

In Chapter 2.1.2, it is proposed to calculate the bond energies of 1NN, 2NN, and 3NN at different compositions x of the alloy $Co_{1-x}Al_x$ to examine their composition dependence. Such calculations are performed using a 2*2*2 supercell with atomic configurations based on A2 at x=0.125, DO_3 at x=0.25, B2 and B32 at x=0.5. Chemical ordering energies for 3*3*3 supercell at x=0.037 and x=0.074 are also calculated. Chapter 4.2 consists of equations in which chemical ordering energies are expressed in terms of energies calculated using VASP simulations at different aluminum atom positions at different compositions.

4.3.2.1 1NN, 2NN and 3NN chemical ordering energies for x=4/54 in $Co_{1-x}Al_x$

For x=0.037=2/54 chemical ordering energies are calculated in chapter 4.3.1. For x=0.074=4/54, energies of atomic configurations shown in Fig. 4.4, Fig 4.5, and Fig 4.6, which are used for finding Ω, Ω', and Ω'' equations of $Co_{50}Al_4$ are summarized in Table

4.8. These energy values are from VASP simulations for a particular atomic configuration.

Table 4.8 Energies of the atomic configurations shown in Figures 4.4, 4.5, and 4.6

	E_6	E_7	E_8	E_9
Energy eV	-367.47519735	-367.92665406	-367.50761878	-368.3818368

From Eq. 4.23 and calculated energies E_6 and E_7, 1NN chemical ordering energy value for $Co_{50}Al_4$ is $\Omega = -0.225728$. Using Eq. 4.29, energy values E_9 and E_6, and $\Omega = -0.225728$ the 3NN chemical ordering energy value is calculated as $\Omega'' = 0.001864$. From Eq. 4.26, energy values E_8 and E_6, and Ω'' , 2NN chemical ordering energy is calculated as $\Omega' = -0.014347$.

4.3.2.2 1NN, 2NN and 3NN chemical ordering energies for x=2/16 in $Co_{1-x}Al_x$

For x=0.125=2/16, energies of atomic configurations shown in Fig. 4.7 are calculated using VASP simulations of 2*2*2 supercell $Co_{14}Al_2$, which is a disordered A2 structure. The energies are summarized in Table 4.9.

Table 4.9 Energies of atomic configurations shown in Fig. 4.7

	E_{10}	E_{11}	E_{12}	E_{13}	E_{14}
Energy eV	-111.993176	-109.738265	-106.965890	-107.506954	-107.510952

Using Eq. 4.33 and E_{10}, E_{11}, and E_{12}, 1NN chemical ordering energy is calculated as $\Omega = -0.258732$, From Eq. 4.37 and energies E_{10}, E_{11}, and E_{13}, 2NN chemical ordering energy is calculated as $\Omega' = 0.004$, From Eq. 4.41 and energies E_{10}, E_{11}, and E_{14}, 3NN chemical ordering energy is calculated as $\Omega'' = 0.002$.

4.3.2.3 1NN, 2NN and 3NN chemical ordering energies for x=4/16 in $Co_{1-x}Al_x$

For x=0.25=4/16, energies of atomic configurations shown in Fig. 4.8 are calculated using VASP simulations for the 2*2*2 supercell. The energy values are summarized in Table 4.10.

Table 4.10 Energies of atomic configurations shown in Fig. 4.8

	E_{15}	E_{16}	E_{17}	E_{18}
Energy eV	-103.40900568	-101.73251376	-103.20049519	-103.25034056

Solving Eq. 4.44, Eq. 4.47, and Eq. 4.50 using energy values from Table 4.10, 1NN, 2NN, and 3NN chemical ordering energy values are calculated as $\Omega = -0.304338$, $\Omega' = -0.0447558$ and $\Omega'' = -0.00623067$ for $Co_{12}Al_4$.

4.3.2.4 1NN, 2NN and 3NN chemical ordering energies for x=8/16 in $Co_{1-x}Al_x$

For x=0.5=8/16, energies of atomic configurations shown in Fig. 4.9 B2 phases and Fig. 4.10 B32 phases are calculated using VASP simulations for 2*2*2 supercell. The energy values are summarized in Table 4.11.

Table 4.11 Energies of atomic configurations shown in Fig. 4.9 and Fig. 4.10

	E_{19}	E_{20}	E_{21}	E_{22}	E_{23}
Energy eV	-95.8983317	-91.7701633	-87.7594779	-87.7866364	-87.3804092

Solving Eq. 4.53, Eq. 4.56, and Eq. 4.59 1NN, 2NN, and 3NN chemical ordering energies are calculated as $\Omega = -0.429491$, $\Omega' = -0.113189$ and $\Omega'' = -0.021935$ for Co_8Al_8.

Calculated 1NN, 2NN, and 3NN chemical ordering energies **Ω**, **Ω'**, and **Ω''** for different aluminum compositions (x) in $Co_{1-x}Al_x$ are summarized in Table 4.12.

Table 4.12 1NN, 2NN and 3NN chemical ordering energy values for Al composition x in $Co_{1-x}Al_x$

Aluminum composition (x)	**Ω**	**Ω'**	**Ω''**
0.037	-0.169	0.0456	0.0437

0.074	-0.225728	-0.014347	0.001863
0.125	-0.258732	0.004	0.002
0.25	-0.304338	-0.04476558	-0.00623067
0.5	-0.429491	-0.113189	-0.021935

The chemical ordering energies are plotted in Fig. 4.12 against aluminum composition (x). A strong composition dependence is observed for the chemical ordering energies of 1NN, 2NN, and 3NN bonds.

Compared to 1NN and 2NN bonds, the 3NN chemical ordering energy becomes less important with increasing composition. On the other hand, the dominant 1NN chemical ordering energy becomes increasingly more important with increasing composition, favoring B2 and DO_3 ordering. At the same time, the 2NN chemical ordering energy changes sign at around x=0.11 from positive to negative and increases in magnitude with increasing composition, favoring DO_3 ordering. As a result, DO_3 is favored for composition around x=0.25 and B2 is favored around x=0.5. Since B32 ordering requires near-zero 1NN chemical ordering energy, it is not favored in β-CoAl alloys.

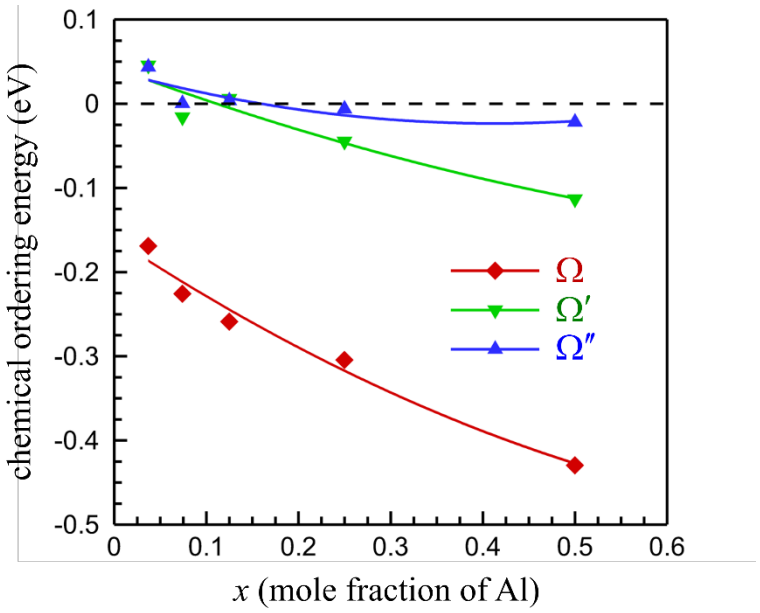

Figure 4.12. Composition dependence of chemical ordering energies Ω, Ω′, Ω″ of 1NN, 2NN, 3NN bonds, respectively, in β-$Co_{1-x}Al_x$ substitutional solid solution.

4.3.3 Elastic Energy from Vegard's Plot of β-CoAl Solid Solutions

In Chapter 2.2.1, it is proposed to calculate the lattice parameters of the $Co_{1-x}Al_x$ solid solutions at different compositions and fit the data to Vegard's law to determine atomic radius misfit between Co and Al atoms and also to determine misfit strain. Figure 4.13 plots the lattice parameter a(x) in the composition range $0.25 \leq x \leq 0.5$, which is relevant to the β-CoAl alloys shown in the phase diagram in Fig. 1.1. Lattice parameters calculation and lattice parameters for different compositions of β-CoAl alloys is shown in Chapter

4.1. The results in Fig. 4.13 show that Vegard's law holds well. To calculate the equilibrium lattice parameters of disordered solid solutions using the supercell method, multiple random configurations at each composition are simulated, and their average values are taken as the lattice parameter at a particular composition which improves the statistics and reduces the errors. According to Eq. (3.9), the misfit strain is determined by the lattice parameter $a_{Co} = a(x = 0)$ and the derivative da/dx, which are respectively the intercept and slope of the fitted straight line in Fig. 4.13. From the linear plot in Fig. 4.13 $a_{Co} = 2.7816$ Å and da/dx = 0.2572 Å, both these value gives misfit stain value $\varepsilon^0 = \frac{a_{Co}^{-1} da}{dx} = 0.0925$.

The lattice parameter of pure Co body-centered cubic crystal is also calculated, which is 2.813 Å and also plotted in Fig. 4.13. As shown in the phase diagram Fig. 1.1, pure Co has a hexagonal close-packed crystal structure (ε-Co) near room temperature and a face-centered cubic crystal (α-Co) at elevated temperature, thus the body-centered cubic crystal structure considered here is unphysical and its result is for comparison purpose only. To be consistent with the micro elasticity theory [28] and Vegard's law [20] in Eq. 3.8 that holds well for the β-CoAl alloys in the composition range $0.25 \leq x \leq 0.5$, the extrapolated lattice parameter $a_{Co} = 2.7816$ Å is used here and also for chemical bond energy calculations.

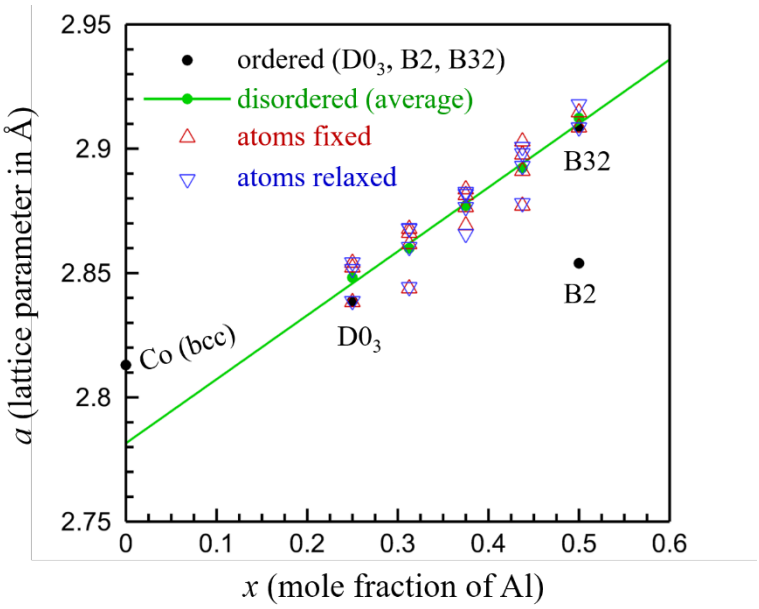

Figure 4.13. Lattice parameter as a function of the composition of $Co_{1-x}Al_x$ solid solutions.

VASP simulations for calculating the lattice parameters of $Co_{1-x}Al_x$ using 2*2*2 supercell, two structural optimization schemes are employed and the results are compared. In one scheme, the atomic positions (i.e., fractional coordinates) in the supercells are fixed; while in another scheme, the atoms are allowed to deviate from their ideal positions during structural relaxation. The calculated lattice parameters are plotted by different colored symbols in Fig. 4.13. It is observed that the two schemes produce consistent results without systematic differences.

Figure 4.14 plots the calculated bulk modulus for the three ordered phases, namely, DO_3 at x=0.25, B2, and B32 at x=0.5. Again, for comparison purposes only, the bulk modulus

of unphysical pure Co of body-centered cubic crystal is also calculated and plotted in Fig.4.14. It shows a general trend that the bulk modulus of β-CoAl alloys decreases with increasing aluminum content. This trend can also be attributed to a general phenomenon observed in DFT calculations that the calculated elastic modulus decreases with increasing lattice parameters. In particular, at the same composition x=0.5, the B2 phase has a smaller lattice parameter and thus a greater bulk modulus than the B32 phase.

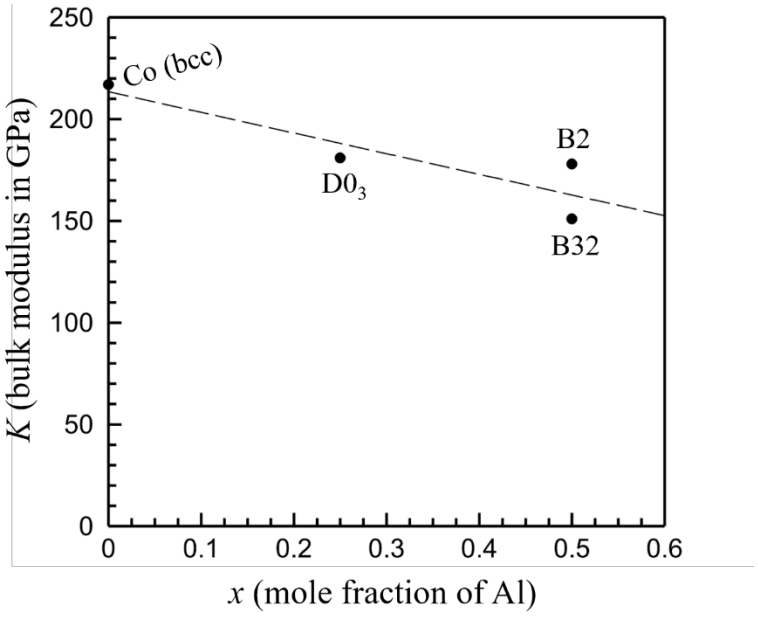

Figure 4.14. Bulk modulus as a function of the composition of $Co_{1-x}Al_x$ solid solutions. The dashed line serves as a guide to the eye.

The elastic energy can be calculated by using Eq. (3.10). The volume per atom is $V = a^3/2$. The reference state lattice parameter $a_{Co} = 2.7816$ Å gives $V = 10.761$ Å^3. Using misfit strain $\varepsilon^0 = 0.0925$, a typical bulk modulus $K = 200$ GPa, and a typical Poisson's ratio $\nu = 0.33$, the elastic energy coefficient is

determined by: $c''' = 3V\left(1-2\nu\right)K\varepsilon_0^2 \big/ \left(1-\nu\right) = 0.175$ eV. This value is compared to the chemical ordering energies in Table. 4.7 and chemical energy coefficients in Table. 4.8. Both comparisons show that the elastic energy contribution is 103.6% compared to 100% of 1NN chemical ordering energy and 12.9% compared to 100% of 1NN chemical energy coefficient, both values are significant.

4.3.4 Lattice Parameters of Ordered and Disordered Solid Solutions

In Chapter 2.3, it is proposed to calculate the lattice parameters of ordered solid solutions and compare them with that of disordered solid solutions at the same composition. Within the composition range $0.25 \leq x \leq 0.5$, DO_3, B2, and B32 are the ordered phases formed. Using two schemes fixed and relaxed, the same lattice parameters are produced at each stoichiometric composition, because atoms in the ordered phase do not relax due to the symmetry of ordered atomic arrangement. The results are also plotted in Fig. 4.13. It shows that DO_3 ordering affects the lattice parameter slightly, B2 ordering changes the lattice parameter significantly, while B32 ordering does not affect the lattice parameter.

The effect of ordering on lattice parameters can be understood from the changes in the 1NN atomic bonds as summarized in Table 4.13. Fig. 4.15 shows atomic configurations at x=0.25 in $Co_{1-x}Al_x$.

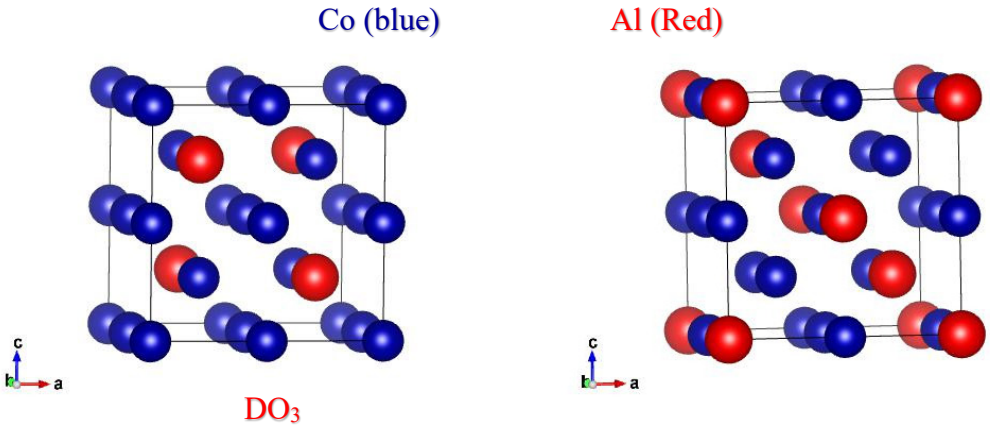

Figure 4.15 Atomic configuration for x=0.25 in $Co_{1-x}Al_x$ using 2*2*2 supercell. One is the ordered phase DO_3 and the other is a disordered phase.

From Fig. 4.15 for the disordered phase at x=0.25, there are 4.5 Co-Co, 0.5 Al-Al, and 3 Co-Al 1NN bonds per atom, while 4 Co-Co bonds, 0 Al-Al bonds, and 4 Co-Al bonds per atom in ordered DO_3 phase. Comparing the two phases considered at x=0.25, the changes in 1NN bonds caused by DO_3 ordering are -0.5 Co-Co bonds, -0.5 Al-Al bonds, and +1 Co-Al bonds per atom. Table 4.13 shows the lattice parameters of ordered DO_3 and disordered phase considered for 1NN atomic bonds calculation.

Table 4.13 Lattice parameters at x=0.25 in $Co_{1-x}Al_x$ for DO_3 ordered phase and disordered phase

Phase	Lattice parameter
DO_3	2.838709
Disordered	2.85407

Atomic configurations considered for 1NN atomic bonds calculations at x=0.5 in $Co_{1-x}Al_x$ for two ordered phases B2 and B32 and one disordered phase are shown in Fig. 4.16

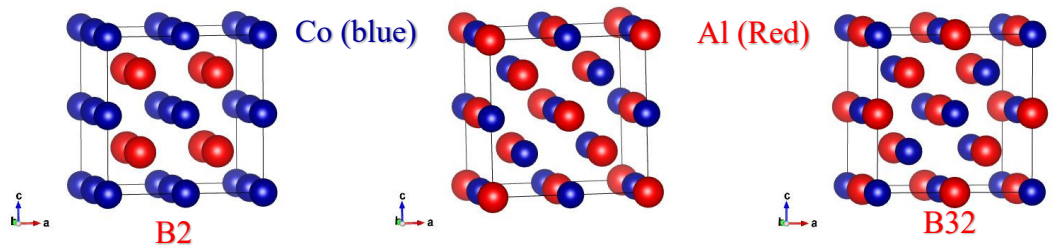

Figure 4.16 Atomic configurations at x=0.5 in $Co_{1-x}Al_x$ for 1NN atomic bonds calculation for B2, disordered phase, and B32.

Lattice parameters of the phases considered for 1NN atomic bond calculations for x=0.5 in $Co_{1-x}Al_x$ are shown in Table 4.14.

Table 4.14 Lattice parameters of x=0.5 in $Co_{1-x}Al_x$ for two ordered phases and one disordered phase considered for 1NN atomic bond calculation

Phase	Lattice parameter
B2	2.85390327
Disordered phase	2.91
B32	2.9085

At x=0.5 in $Co_{1-x}Al_x$ for the disordered phase considered, there are 2 Co-Co, 2Al-Al, and 4 Co-Al 1NN bonds per atom. For the B2 phase, there are 0 Co-Co, 0Al-Al, and 8 Co-Al 1NN bonds per atom. The change in the bonds caused by B2 ordering is -2 Co-Co bonds, -2 Al-Al bonds, and +4 Co-Al bonds per atom, which is 4 times the change in the case of DO_3 ordering. In contrast, there are 2 Co-Co bonds, 2 Al-Al bonds, and 4 Co-Al bonds per atom in the ordered B32 phase. B32 ordering does not cause changes in the bonds. B2 ordering however decreases the lattice parameter significantly from 2.91 Å to 2.8539 Å (-1.93%), DO_3 ordering slightly decreases the lattice parameter from 2.854 Å to 2.8387 Å (-0.536%), while B32 ordering change the lattice parameter from 2.91 Å to 2.9085 Å, (-0.055%) within the inaccuracy of DFT calculation.

Table 4.15 The changes in the numbers of 1NN atomic bonds caused by ordering.

ordering	change in the number of 1NN bonds per atom		
	Co-Co	Al-Al	Co-Al
$D0_3$	-0.5	-0.5	+1
B2	-2	-2	+4
B32	0	0	0

The foregoing observation implies that the lattice parameter is determined by the 1NN atomic bonds. In particular, the Co-Al 1NN bond has a shorter length than the average length of Co-Co and Al-Al 1NN bonds. Since B32 ordering does not affect the number of the 1NN bonds, B32 ordering must be driven by the 2NN bonds as well as the bonds of longer atomic distances.

Using 3*3*3 supercell, equilibrium lattice parameters for x=0.037=2/54 in $Co_{1-x}Al_x$ i.e., $Co_{52}Al_2$ are calculated with Al atoms in 1NN, 2NN, and 3NN atomic positions. Equilibrium lattice parameters of corresponding Al positions are tabulated in Table 4.16.

Table 4.16 Equilibrium lattice parameters of $Co_{52}Al_2$ with Al atoms in 1NN, 2NN and 3NN positions

Al atom positions	Equilibrium lattice parameter
1NN	2.816994694
2NN	2.816149137
3NN	2.816247

Equilibrium lattice parameters of $Co_{52}Al_2$ are plotted against Al-Al bond distance in 1NN, 2NN, and 3NN. Fig. 4.17 depicts the dependence of lattice parameters on Al-Al bond distance in 1NN, 2NN, and 3NN positions.

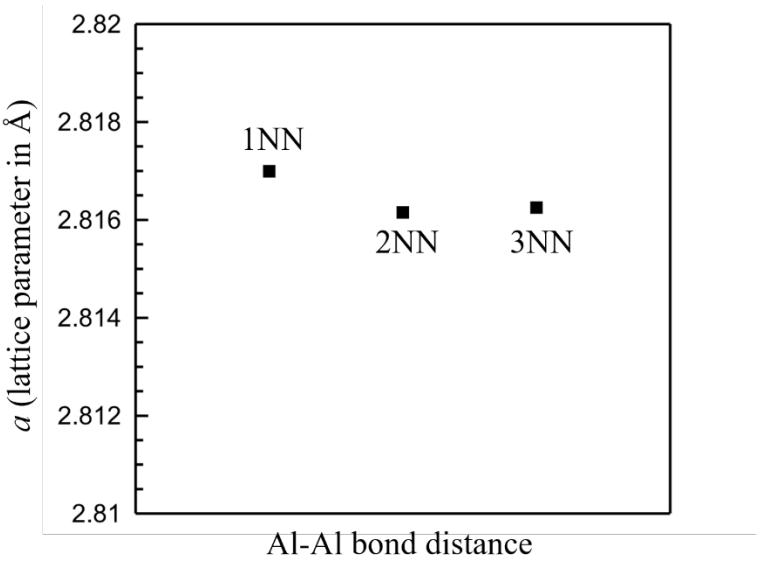

Figure 4.17. Dependence of the lattice parameter of $Co_{52}Al_2$ solid solution on Al-Al bond distance, namely, 1st, 2nd, and 3rd nearest neighbor, respectively.

The lattice parameters are determined by the 1NN atomic bonds and the Co-Al 1NN bond has a shorter bond length than the average length of Co-Co and Al-Al 1NN bonds is further supported by the calculated lattice parameters of $Co_{52}Al_2$ solid solution for three different Al-Al bond distances, namely, 1NN, 2NN and 3NN, respectively, as shown in Fig. 4.17. In particular 1NN bond has a longer bond length leading to a slightly larger lattice parameter (note the very dilute Al concentration in the 3*3*3 supercell), while the Al-Al 2NN and 3NN bonds do not affect the lattice parameter.

5 Conclusion and Future Work

For β-$Co_{1-x}Al_x$ substitutional solid solution, the 2NN and 3NN chemical bond energies are significant compared to 1NN chemical bond energy. The solid solution requires consideration of chemical bonds beyond 1NN which include 2NN and 3NN bond energies. The chemical ordering energies of 1NN, 2NN, and 3NN bonds in Co-Al substitutional solid solution depends on the alloy composition. For x=0.25 in β-$Co_{1-x}Al_x$ DO_3 ordering is favored, at x=0.5 B2 ordering is favored and B32 ordering is not favored in β-CoAl alloys. Vegard's law holds well in disordered β-$Co_{1-x}Al_x$ substitutional solid solutions and the atomic radius misfit between Al solute atoms and Co solvent atoms produces a misfit strain $\varepsilon^0 = 0.0925$ and elastic energy per solute atom 0.175 eV. The elastic energy is significant in comparison to chemical bond energies and thus must be taken into account. Atomic ordering affects the lattice parameter and the lattice parameter is determined by 1NN atomic bonds. Atomic ordering is determined by 1NN, 2NN, and 3NN atomic bonds.

6 References

[1] H. Masumoto, T. Kobayashi and K. Watanabe, "On a New Magnet Alloy "Malcolloy" in the System of Cobalt and Aluminum," *Trans. Japan. Inst. Metals,* vol. 6, pp. 187-191, 1965.

[2] J. Frenkel and J. Dorfman, "Spontaneous and Induced Magnetization in Ferromagnetic Bodies," *Nature,* vol. 126, no. 3173, pp. 274-275, 1930.

[3] J. Livingston, "Microstructure and Coercivity of Permanent-Magnet Materials," *Prog. Mater. Sci,* vol. Chalmers Anniversary Volume, pp. 243-268, 1981.

[4] Livingston, J. D., "Microstructure and properties of Rare Earth Magnets," *(Schenectady, New York: General Electric Company, 1986).*

[5] A. J. Schwartz, "The Interrelationship between Microstructure, Coercivity and Magnetic Viscosity in Co-Al and Co-Ni-Al Fine-Particle Ferromagnets," *Department of Materials Science and Engineering, School of Engineering, University of Pittsburgh,* 1991.

[6] A. Zeltser and W. Soffa, "Magnetic Hardening in Co-Al Alloys," *IEEE Transactions on Magnetics,* Vols. Mag-22,N0.5, pp. 588-590, 1986.

[7] A. Schwartz and W. Soffa, "Decomposition of Beta-Phase Co-Al Alloys: Precipitate Crystallography and Morphology," *Scripta Metallurgica et Materialia,* vol. 25, pp. 185-190, 1991.

[8] A. Zeltser, "The Decomposition of β-CoAl Alloys and Relationship between the Microstructure and Coercivity," *Ph.D. Thesis, University of Pittsburgh,* 1988.

[9] R. Evans, W. Fan, P. Chureemart, T. Ostler, M. Ellis and R. Chantrell, "Atomistic Spin Model Simulations of Magnetic Nanomaterials," *Journal of Physics: Condensed Matter,* vol. 26, 2014.

[10] A. Hubert and R. Schafer, "Magnetic Domains: The Analysis of Magnetic Microstructures," *Springer Science & Business Media, Berlin,* 1998.

[11] X. Xuo, "Atomistic Monte Carlo Simulation Study of Phase Transitions in Metal Alloys," *Ph.D. Thesis, Michigan Technological University,* 2021.

[12] M. Hansen and K. Anderko, Constitution of Binary Alloys (2nd edition), New York: McGraw-Hill, 1958.

[13] J. Schramm, "The Binary System Cobalt-Aluminum," *Z. Metallik.,* vol. 33, pp. 381-387, 1941.

[14] B.-J. Lee and M. Baskes, "Second nearest-neighbor modified embedded-atom-method potential," *Phys. Rev. B,* vol. 62, 2000.

[15] B. Lee, M. Baskes, H. Kim and Y. Cho, "Second Nearest-Neighbor Modified Embedded Atom Method Potentials for BCC Transition Metals," *Physical Review B,* vol. 64, 2001.

[16] C. Zhiwei, G. Feng, C. Zhihua and Q. Jianmin, "A Second Nearest-Neighbor Embedded Atom Method Interatomic Potential for Li-Si Alloys," *Journal of Power Sources,* vol. 207, pp. 150-159, 2012.

[17] G.-U. Jeong, C. S. Park, H.-S. Do, S.-M. Park and B.-J. Lee, "Second Nearest-Neighbor Modified Embedded-Atom Method Interatomic Potentials for the Pd-M (M= Al, Co, Cu, Fe, Mo, Ni, Ti) Binary Systems," *Calphad,* vol. 62, pp. 172-186, 2018.

[18] S. Wohlthat, J. R. Reimers and N. S. Hush, "Accurate and Computationally Efficient Third-Nearest-Neighbor Tight-Binding Model for Large Graphene Fragments," *Physical Review N,* vol. 81, 2010.

[19] W. A. Soffa, D. E. Laughlin and N. Singh, "Interplay of Ordering and Spinodal Decomposition in the Formation of Ordered Precipitates in Binary FCC Alloys: Role of Second Nearest-Neighbor Interactions," *Philosophical Magazine,* vol. 90, pp. 287-304, 2010.

[20] L. Vegard and Z. Kristallogr, *Z.Phys.,* vol. 67, p. 239, 1928.

[21] W. Hume-Rothery, R. Smallman and C. Hayworth, "The Structure of Metals and Alloys," *The Metals and Metallurgy Trust, London,* 1969.

[22] J. L. Barrat, M. Baus and J. Hansen, "Freezing of Binary Hard-Sphere Mixtures into Disordered Crystals: A Density Functional Approach," *Journal of Physics C,* vol. 20, p. 1413, 1987.

[23] H. J. Axon and W. Hume-Rothery, in *Proc. R. Soc.*, London, 1948.

[24] A. R. Denton and N. W. Ashcroft, "Vegard's Law," *Physical Review A,* vol. 43, p. 3161, 1991.

[25] T. Uesugi and K. Higashi, "First-Principles Studies on Lattice Constants and Local Lattice Distortions in Solid Solution Aluminum Alloys," *Comput. Mater. Sci,* vol. 67, pp. 1-10, 2013.

[26] T. Uesugi, Y. Takigawa and K. Higashi, "Deformation Mechanism of Nanocrystalline Al-Fe Alloys by Analysis from Ab-Initio Calculations," *Materials Science Forum,* Vols. 503-504, pp. 209-214, 2006.

[27] I. Kim, H. Oh, S. Kim and E. Park, "Rapid Assessment of Solid Solution Hardening via Atomic Size Misfit Parameter in Refractory Concentrated Alloys," *Journal of Alloy Compounds,* vol. 886, 2021.

[28] A. Khachaturyan, Theory of Structural Transformations in Solids, New York: John Wiley & Sons, 1983.

[29] Y. Wang and A. Khachaturyan, "Three-Dimensional Field Model and Computer Modeling of Martensitic Transformations," *Acta Materialia,* vol. 45, pp. 759-773, 1997.

[30] J. Zhang and L. Chen, "Phase-Field Microelasticity Theory and Micromagnetic Simulations of Domain Structure in Giant Magnetostrictive Materials," *Acta Materialia,* vol. 53, pp. 2845-2855, 2005.

[31] D. Porter and K. Easterling, Phase Transformations in Metals and Alloys, London: Chapman & Hall, 1992.

[32] P. Hohenberg and W. Kohn, "InhomogeneousElectron Gas," *Physical Review,* vol. 136, p. 864, 1964.

[33] W. Kohn and L. J. Sham, "Perspective on "Self-Consistent Equations Including Exchange and Correlation Effects"," *Physical Review A,* vol. 140, pp. 1133-1138, 1965.

[34] R. F. L. Evans, W. J. Fan, P. Chureemart, T. A. Ostler, M. O. A. Ellis and R. W. Chantrell, "Atomistic Spin Model Simulations of Magnetic Nanomaterials," *Journal of Physics: Condensed Matter,* vol. 26, p. 23, 2014.

[35] T. v. Mourik, M. Buhl and M.-P. Gaigeot, "Density Functional Theory across Chemistry, Physics and Biology," *Philosophical Transactions A,* vol. 372, 2011.

[36] G. Kresse and J. Furthmuller, "Efficient Iterative Schemes for Ab Initio Total-Energy Calculations Usinf a Plane-Wave Basis Set," *Physical Review B,* vol. 54, pp. 11169-11186, 1996.

[37] P. E. Blochl, "Projector Augmented-Wave Method," *Physical Review B: Condensed Matter,* vol. 50, pp. 17953-17979, 1994.

[38] J. Perdew, K. Burke and M. Ernzerhof, "Generalized Gradient Approximation Made Simple," *Phys. Rev. Lett.,* vol. 77, pp. 3865-3868, 1996.

[39] J. D. Pack and H. J. Monkhorst, "Special Points for Brillouin-Zone Integrations - A Reply," *Physical Review B,* vol. 16, pp. 1748-1749, 1977.

[40] M. Mehl, J. Osburn, D. Papaconstantopoulos and B. Klien, "Structural Properties of Ordered High-Melting-Temperature Intermetallic alloys from First-Principles Total Energy Calculations," *Physical Review B,* vol. 41, p. 10311, 1990.

[41] K. Momma and F. Izumi, "VESTA 3 for three-dimensional visualization of crystal, volumetric and morphology data," *J. Appl. Crystallogr.,* vol. 44, pp. 1272-1276, 2011.

[42] K. Hathaway and A. Clark, "Magnetostrictive Materials," *MRS Bulletin,* vol. 18, p. 34, 1993.

[43] A. Clark, "Magnetostrictive rare earth-Fe2 compounds," *Ferromagnetic Materials,* vol. 1, no. edited by E.P. Wohlfarth, North-Holland, p. 531, 1980.

[44] D. Peterson, J. Verhoeven, O. McMasters and W. Spitzig, "Strength of Terfenol-D," *Journal of Applied Physics,* vol. 65, p. 3712, 1989.

A Copyright documentation

All the figures used in this thesis for visualizing the atomic configurations of Co and Al atoms at different compositions in 2*2*2 supercells and in 3*3*3 supercells are produced by using “Visualization for Electronic and Structural Analysis (VESTA) software [41]. It is an open software that is used for three-dimensional visualization of crystal systems. VESTA Version 3 is used for the visualization.

For data analysis, Tecplot 360 2022 R2 is used. Tecplot 360 is an integrated 2D and 3D plotting software used for complete visualization and analysis of simulation and test data.